Fundação
para a Ciência
e a Tecnologia

This work was financially supported by 2024.06584.CERN

The ATLAS High-Granularity Timing Detector for the HL-LHC

Project Status and Results

Helena Santos (LIP)

Why more luminosity?

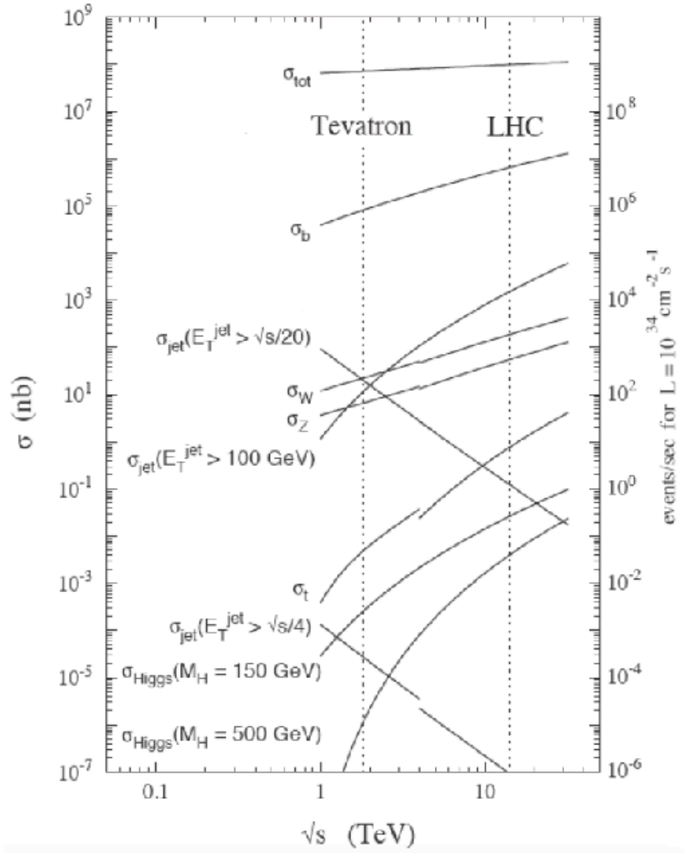

HL-LHC physics goals

Precision tests of the SM at the TeV scale

Precise measurements of Higgs couplings and self-coupling

Rare SM processes

Searches for physics beyond the SM

Higgs as a portal to the dark sector

Why more luminosity?

Snowmass White paper

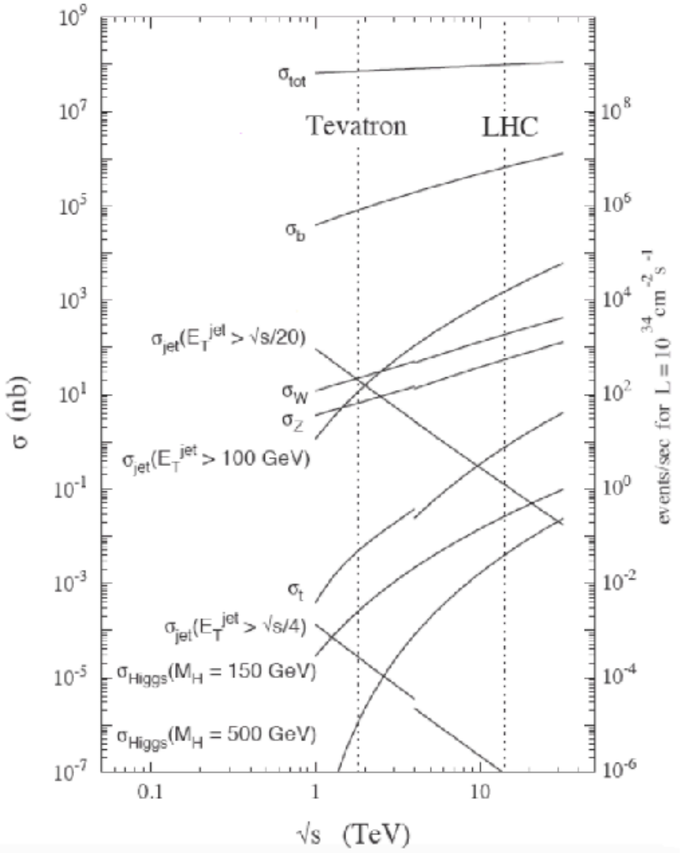

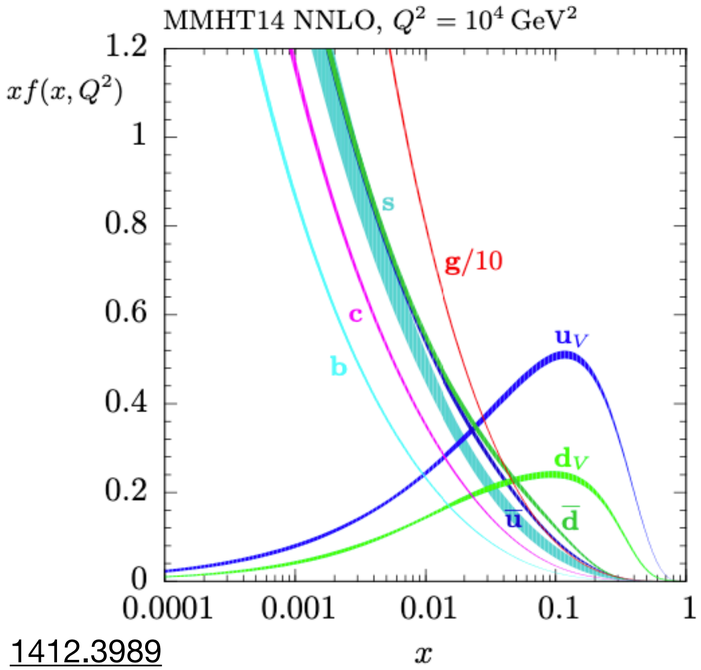

1412.3989

Rare processes probe regions of the phase space with small parton luminosities.
However, at the relevant scales, the proton structure is dominated by low-x gluons and sea quarks

HL-LHC physics goals

Precision tests of the SM at the TeV scale

Precise measurements of Higgs couplings and self-coupling

Rare SM processes

Searches for physics beyond the SM

Higgs as a portal to the dark sector

This poses significant challenges on detectors:

pileup scales linearly with luminosity ($\mu = L\sigma_{ine}/f_{BC}$), while

detector occupancy is driven by the soft-QCD nature of inelastic *pp* interactions, dominated by low-x partons

The collateral effect - pileup

<μ> ~ 200 interactions per bunch crossing pose unprecedented challenges for the detectors if they keep similar performance:

L**arger events:** hundreds of overlapping collisions —> many more tracks and vertices

Higher detector occupancy: requires finer granularity

Higher trigger rates: demands redesigned trigger and readout architecture

Increased reconstruction complexity: more sophisticated online algorithms needed

Severe radiation environment: requires radiation-hard sensors and electronics

Z->μμ candidate event with 65 additional reconstructed vertices from other interactions (μ ~ 90)

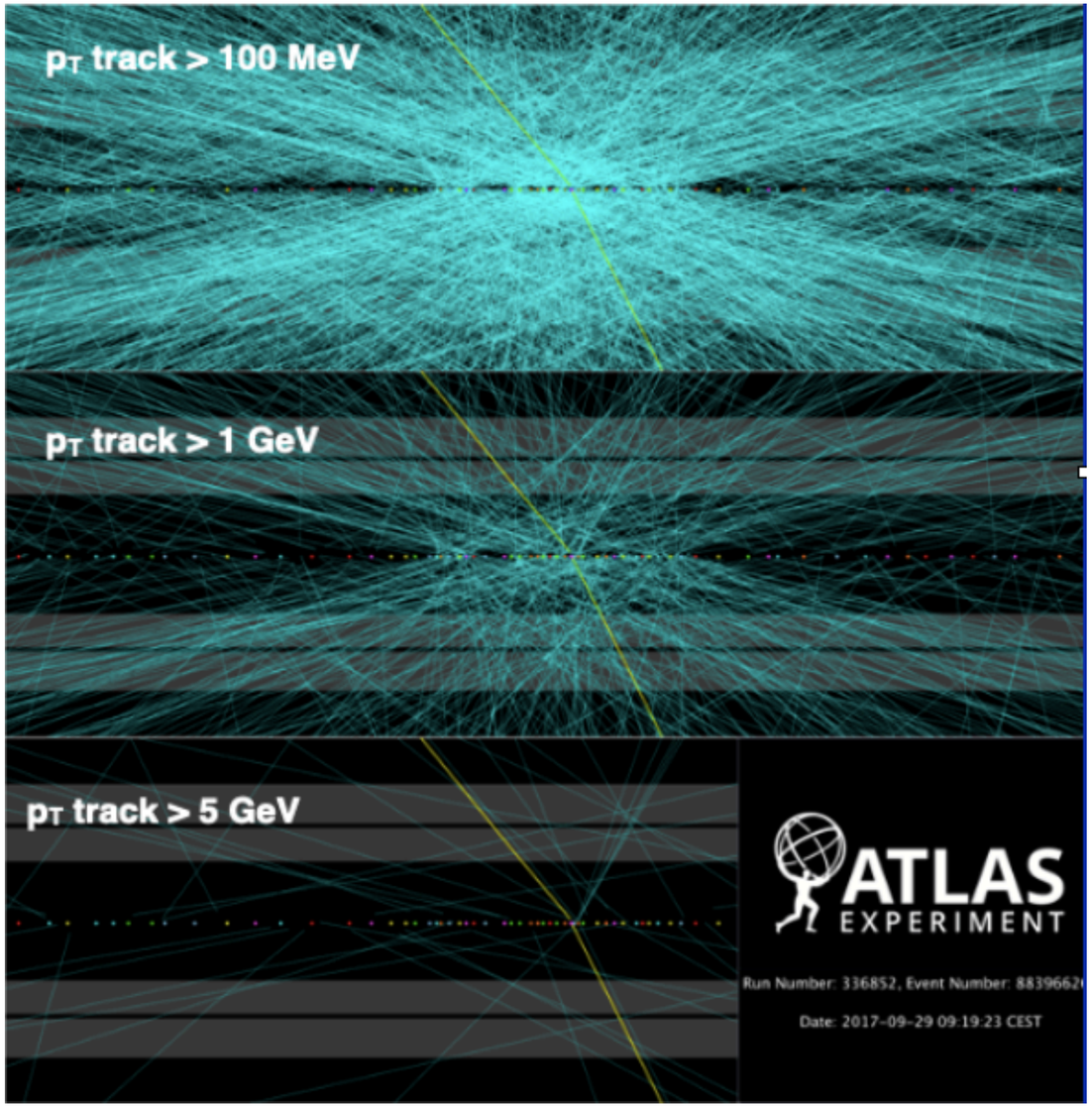

ATLAS Phase-2 upgrade

Trigger and Data Acquisition:

- First level trigger at 1 MHz (today is 100 kHz), 4.6 TB/s
- Event Filter 10 kHz (today is 1 kHz), ~60 GB/s

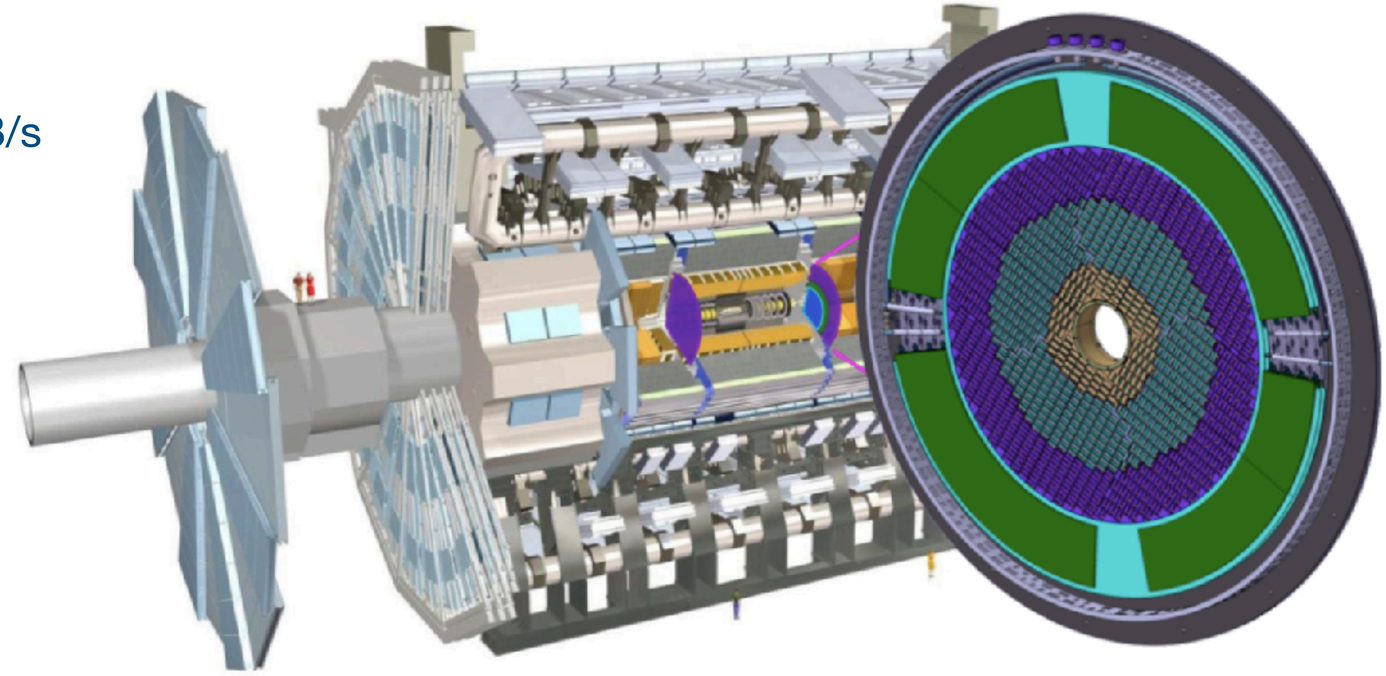

Electronics upgrade:

- Online/Offline-detector electronics for Calorimeters and Muon systems

New Inner Tracker Detector:

- All Silicon
- 9 layers for $|\eta| < 4$
- Reduced material budget
- Finer segmentation

New muons chambers:

- Inner barrel with new RPCs, sMDTs and TGCs
- Improves momentum resolution, trigger efficiency and fake rejection

High Granularity Timing Detector (HGTD):

- Precision timing using Silicon Low Gain Avalanche Detectors (LGAD)
- Improves pileup separation and measures luminosity

Additional upgrades:

- Luminosity detectors (1% precision),
- Zero degree calorimeter for Heavy Ion physics

Upgraded Inner Tracker of ATLAS — ITk

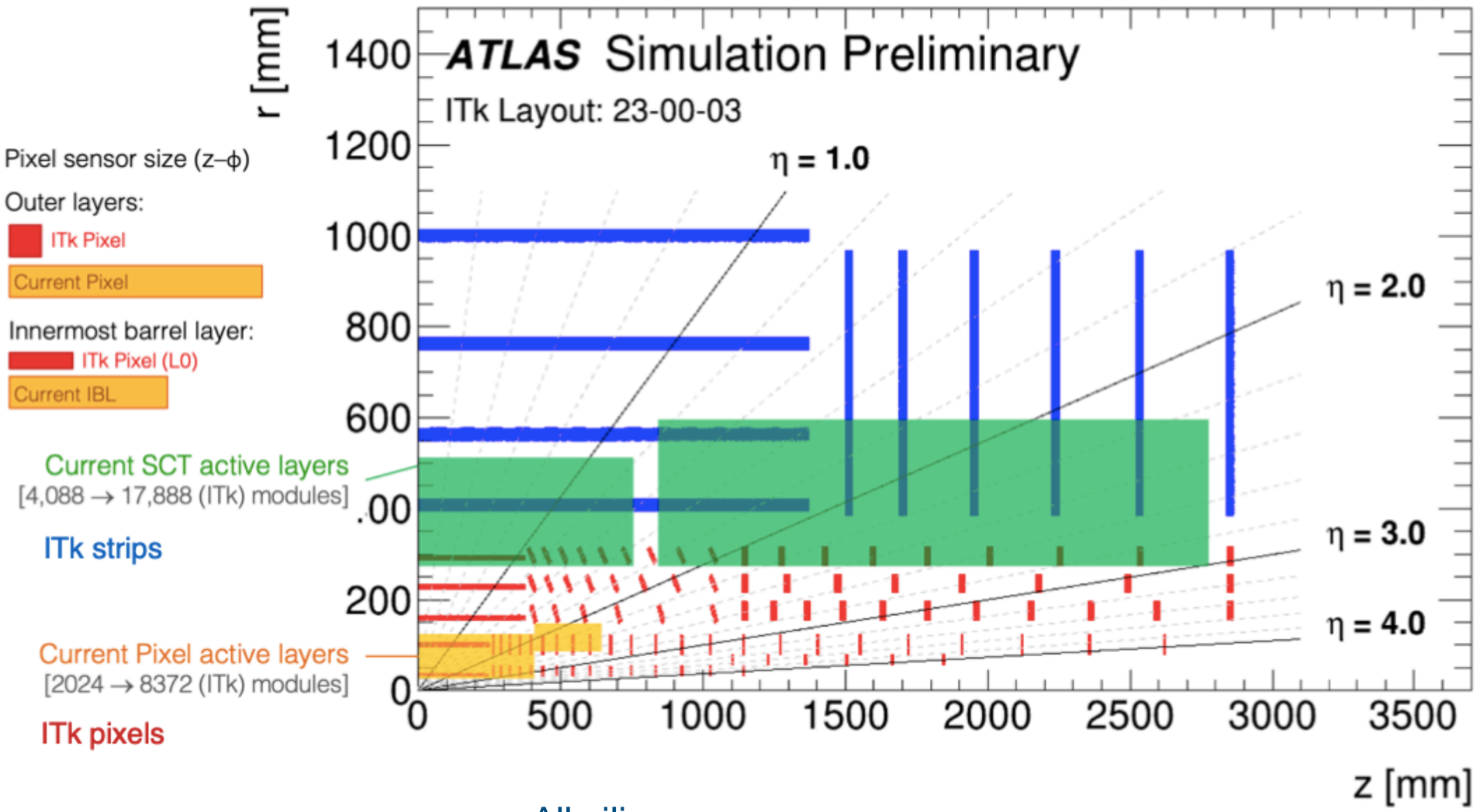

- All silicon
- Finer segmentation
- pseudorapidity coverage increase from 2.5 to 4 units

Why do we need a timing detector in ATLAS

HGTD Public Results

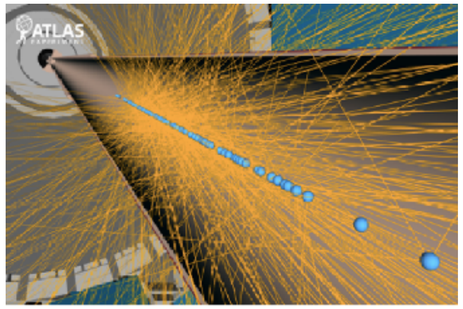

With 200 interactions per bunch-crossing, vertex density will be on average 1.6 vertices/mm

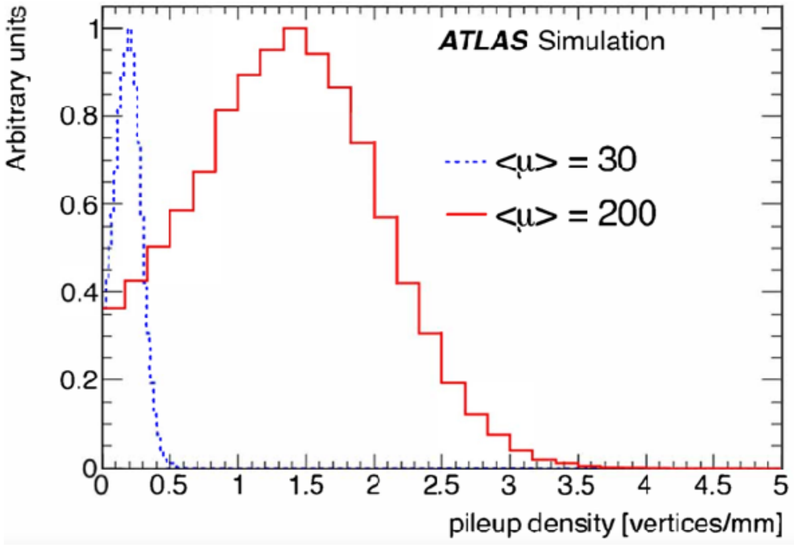

Longitudinal impact-parameter track resolution, $\sigma(z_0)$, worsens at large η

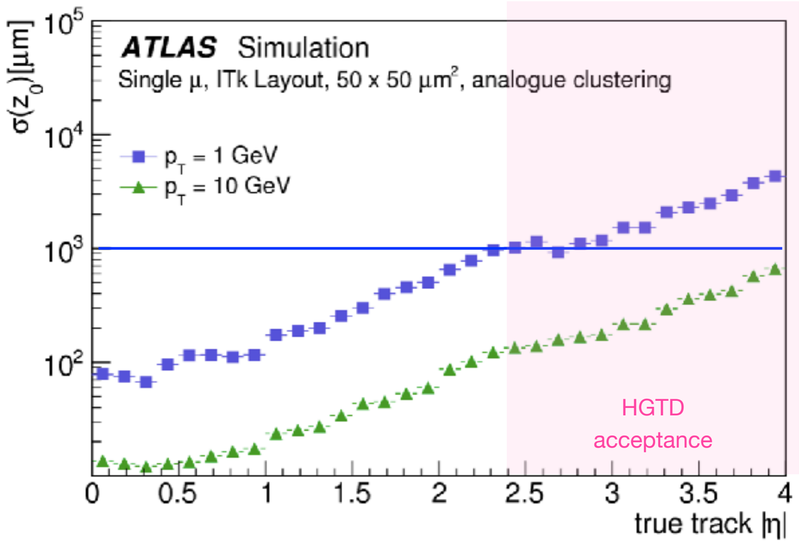

→ Vertex spacing (~0.6 mm) smaller than z_0 resolution in the forward region

→ Reconstructed vertices overlap

→ Tracks from different vertices can be assigned to a given vertex

Ambiguity in track to vertex association

Why do we need a timing detector in ATLAS

HGTD Public Results

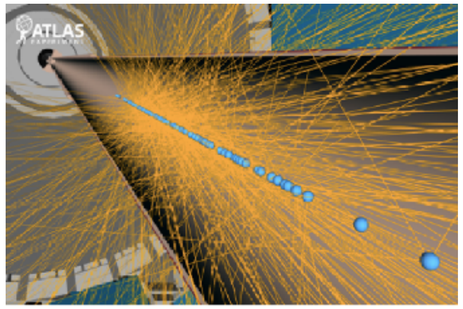

With 200 interactions per bunch-crossing, vertex density will be on average 1.6 vertices/mm

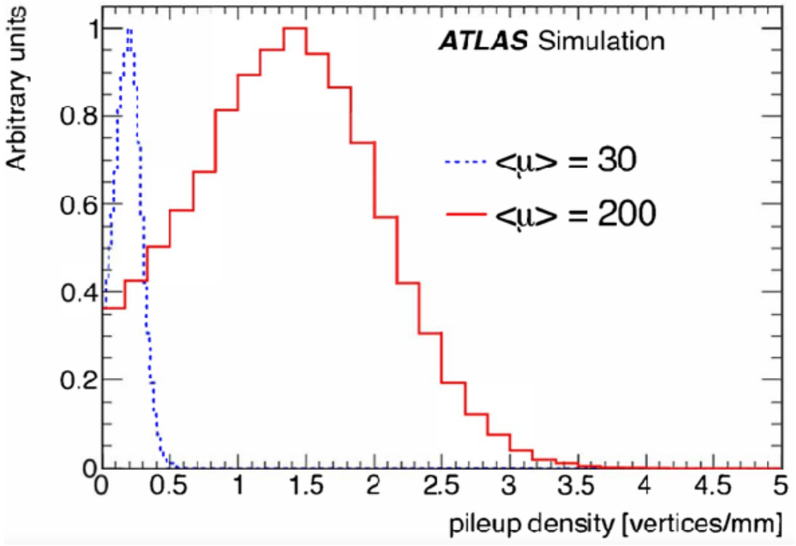

Longitudinal impact-parameter track resolution, $\sigma(z_0)$, worsens at large η

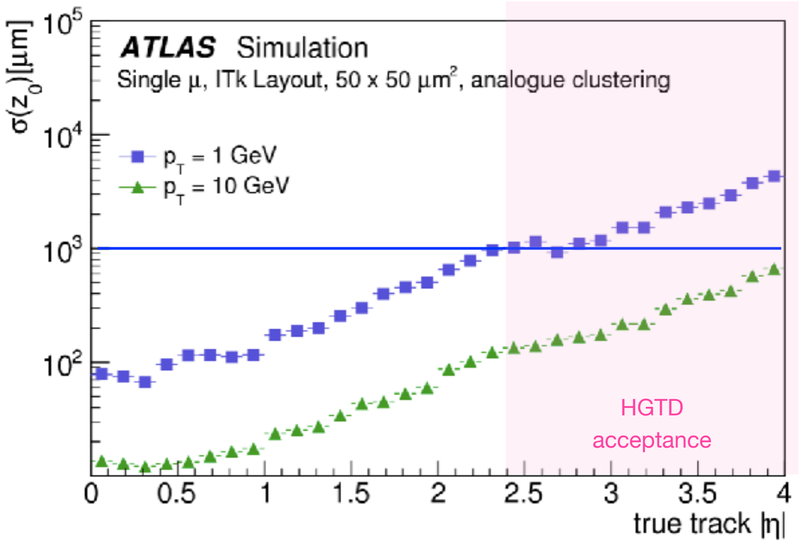

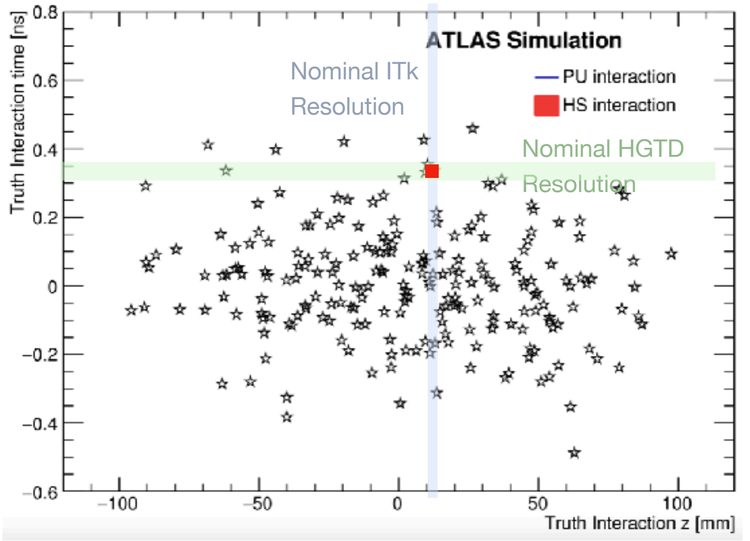

→ Vertex spacing (~0.6 mm) smaller than z_0 resolution in the forward region

→ Reconstructed vertices overlap

→ Tracks from different vertices can be assigned to a given vertex

Ambiguity in track to vertex association

HGTD can associate a time to each track with unprecedented accuracy

It will work if σ_{time} << vertex spread in time is (~180 ps)

Physics performance with HGTD

HGTD Public Results

Efficiency for electrons to pass track-isolation criteria as function of the local vertex density

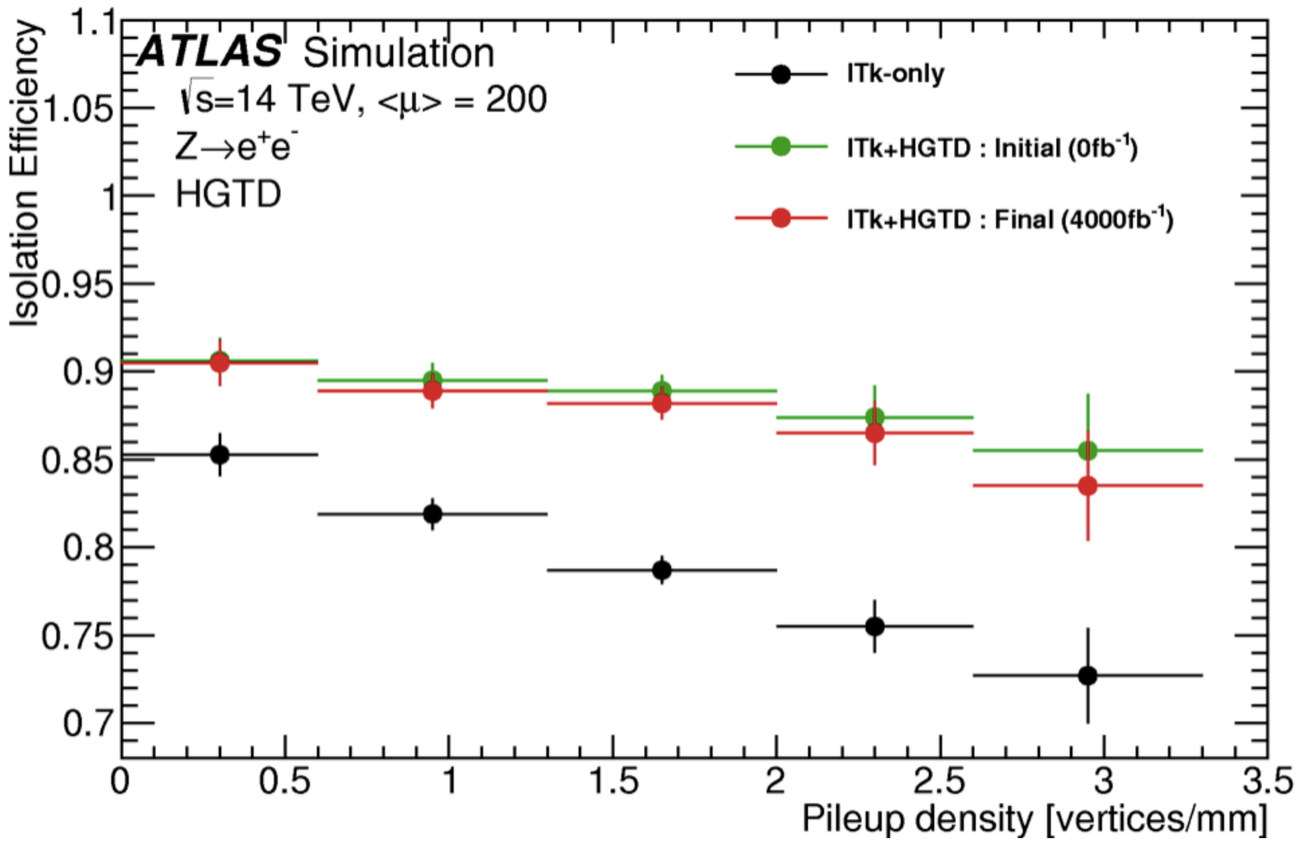

7% — 20% increasing efficiency

The improvement does not degrade significantly at the HGTD end of life

Physics performance with HGTD - Jets

ATL-HGTD-PUB-2022-001

Rejection of pileup dijets as a function of the efficiency of selecting hard-scatter jets

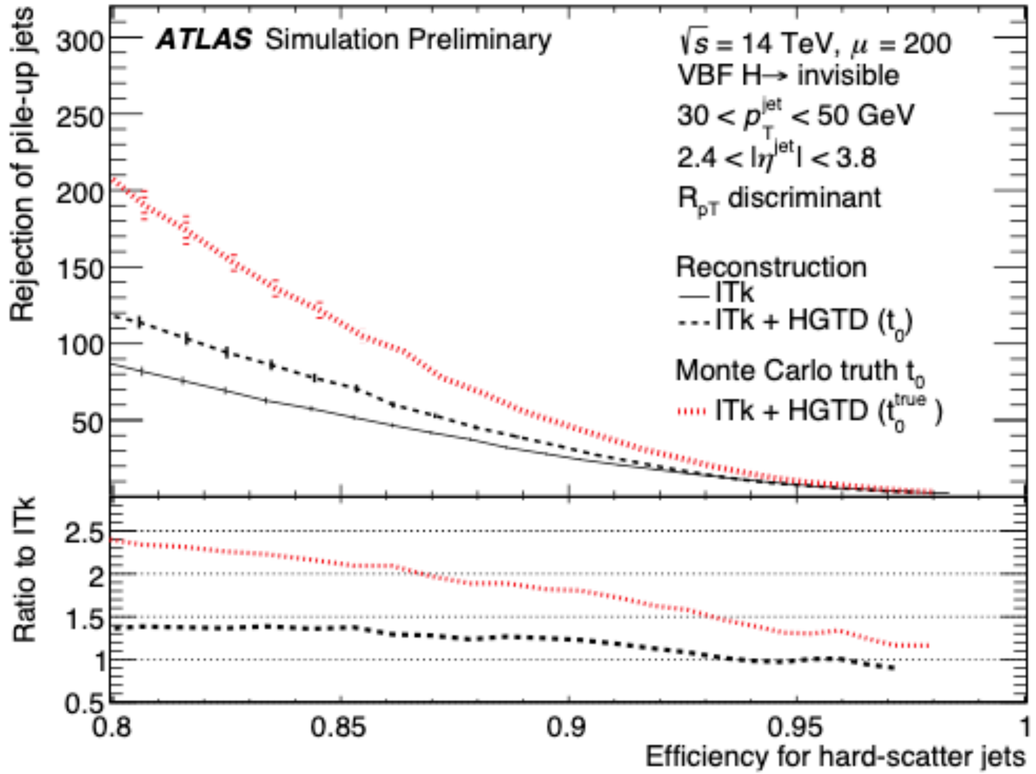

t_0 - reconstructed time of the hard-scatter vertex

Factor 1.5 better than tracker-only at 0.85 working point, with potential for further improvements

HGTD characteristics

Pad detector for precision timing in the forward region of ATLAS:

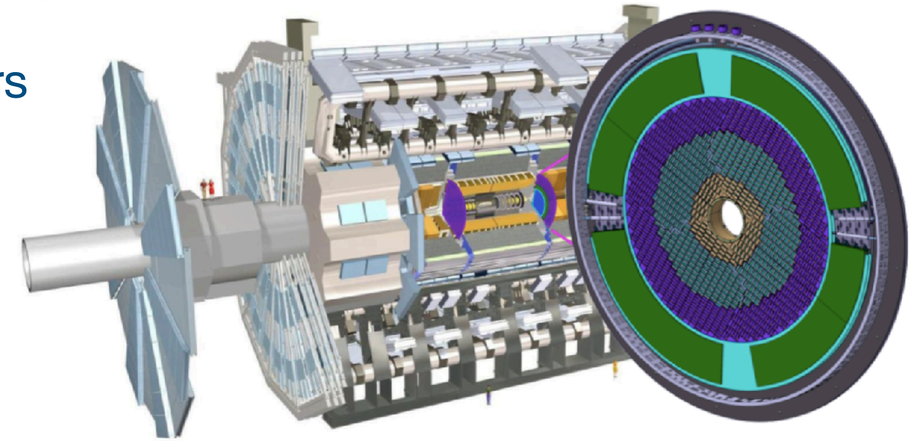

- Two vessels located between the barrel and endcap calorimeters
- Each vessel: two disks with detectors mounted on both sides
- Each disc with 3 rings: inner, middle and outer
- Located at ±3.5 m from the interaction point
- Radial range: 120 mm < r < 640 mm
- Active coverage: 2.4 < |η| < 4
- Radiation hardness:
  - Up to 2.5 × 10^{15} n_{eq}/cm^2
  - 2 MGy total ionising dose (TID)

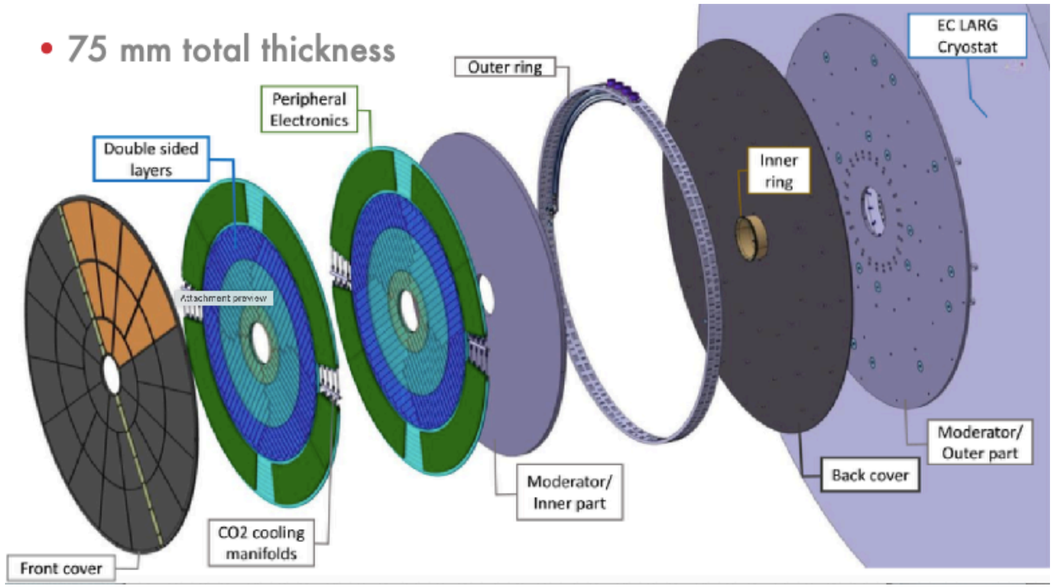

Performance Goals

- Time resolution (per hit): 40–85 ps up to 4000 fb^{-1}
- Time resolution (per track): 30–50 ps up to 4000 fb^{-1}

Luminosity Measurement

- Counts hits at 40 MHz, bunch-by-bunch, with 1% precision

Sensor technology - LGAD

16064 silicon sensors with internal gain based on LGAD (Low Gain Avalanche Diode) technology

Sensor production

- 8-inch silicon substrate (wafer)
- 52 sensor arrays per wafer

Pad & Sensor specifications

- Pad matrix: 15 × 15 = 225 pad per sensor
- Pad size: 1.3 mm × 1.3 mm
- Active thickness: 50 μm
- Total thickness: 775 μm

HGTD design

- Four sensor layers → ensures ≥ 2 hits per track

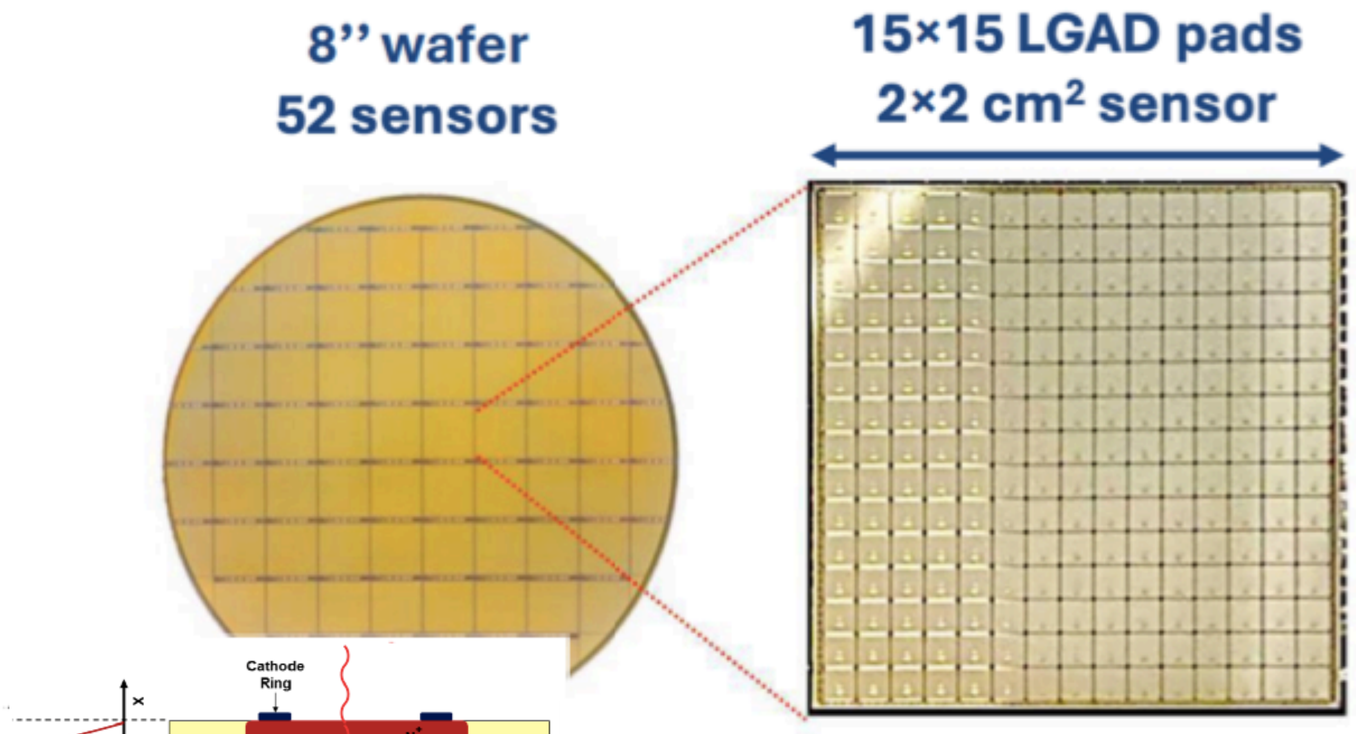

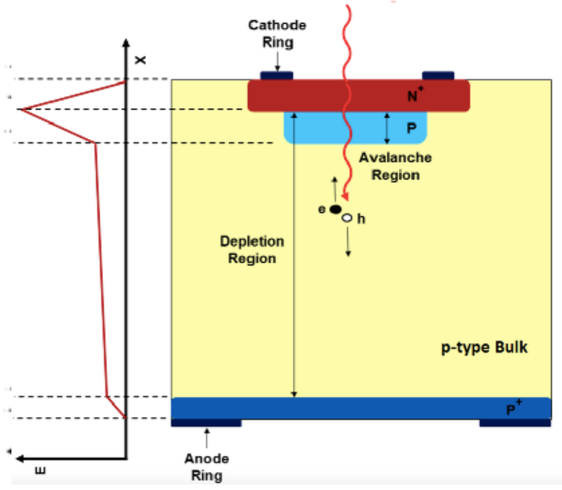

N-on-P diode with
extra p-type gain layer (10-40)
Fast rise time and high signal-to-noise (15-30)
Collected charge/hit: 10 fC (start); 4 fC (EoL)
Hit efficiency: 97% (start); 95% (end)

The ALTIROC module

ATLAS LGAD Timing Integrated ReadOut Chip

- Two readout ASICs bump-bonded to two LGAD sensors, mounted on a PCB for power and communication
- A FLEX tail carrying HV, LV and signals to/from peripheral electronics boards (PEB)
- Per-module HV settings to accommodate the variation of radial fluence

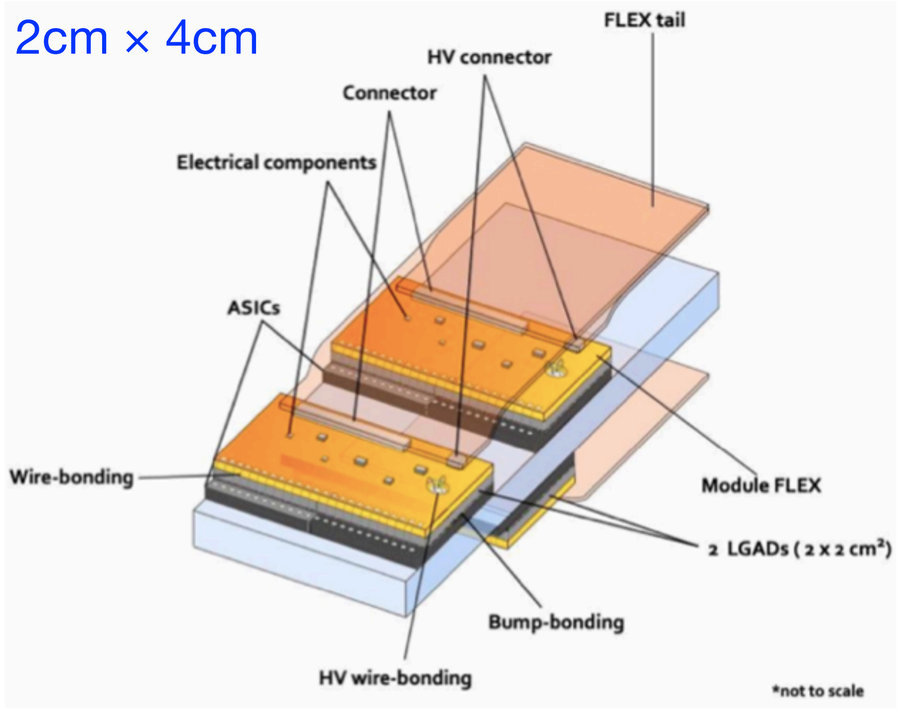

The ALTIROC module

ATLAS LGAD Timing Integrated ReadOut Chip

- Two readout ASICs bump-bonded to two LGAD sensors, mounted on a PCB for power and communication
- A FLEX tail carrying HV, LV and signals to/from peripheral electronics boards (PEB)
- Per-module HV settings to accommodate the variation of radial fluence
- The LGADs will be maintained at -30 °C using an evaporative CO_2 cooling manifold integrated in the disks

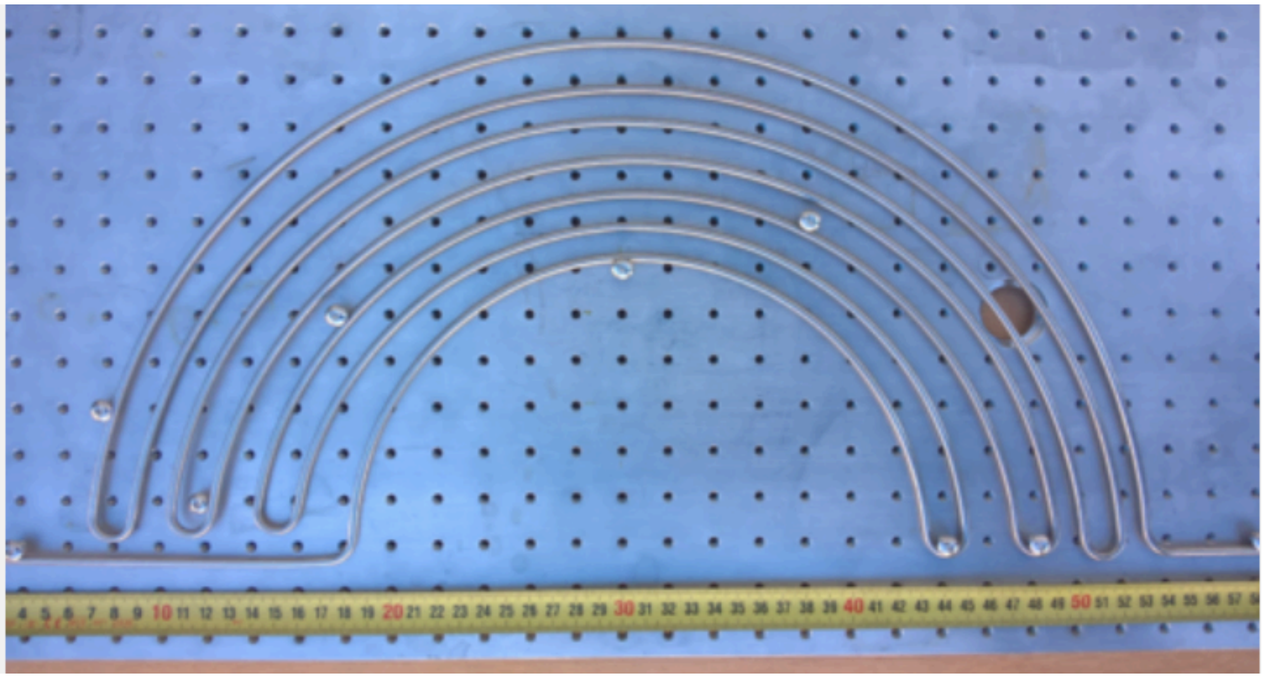

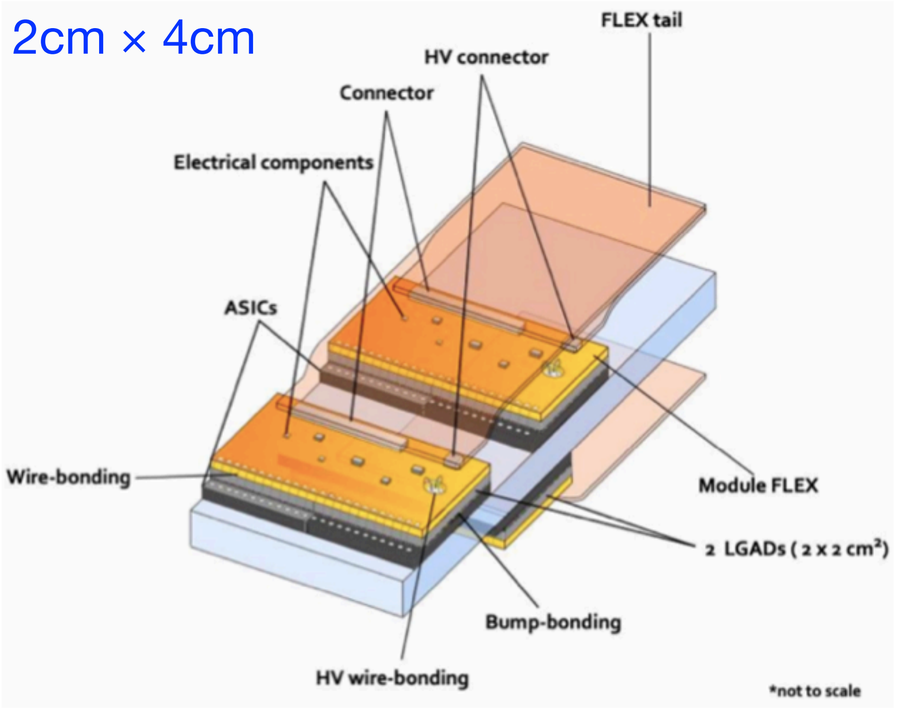

The ALTIROC module

ATLAS LGAD Timing Integrated ReadOut Chip

- Two readout ASICs bump-bonded to two LGAD sensors, mounted on a PCB for power and communication
- A FLEX tail carrying HV, LV and signals to/from peripheral electronics boards (PEB)
- Per-module HV settings to accommodate the variation of radial fluence
- The LGADs will be maintained at -30 °C using an evaporative CO_2 cooling manifold integrated in the disks

Specifications:

- Radiation-Tolerant 130 nm CMOS (TSMC)
- Minimum discriminator threshold: 2 fC
- Front-end jitter: < 25 ps @ 10 fC and < 65 ps @ 4 fC
- HGTD cooling power requirement (20 kW/vessel):
  Overall (sensor) power density: < 300 mW/cm² (100 mW/cm²)

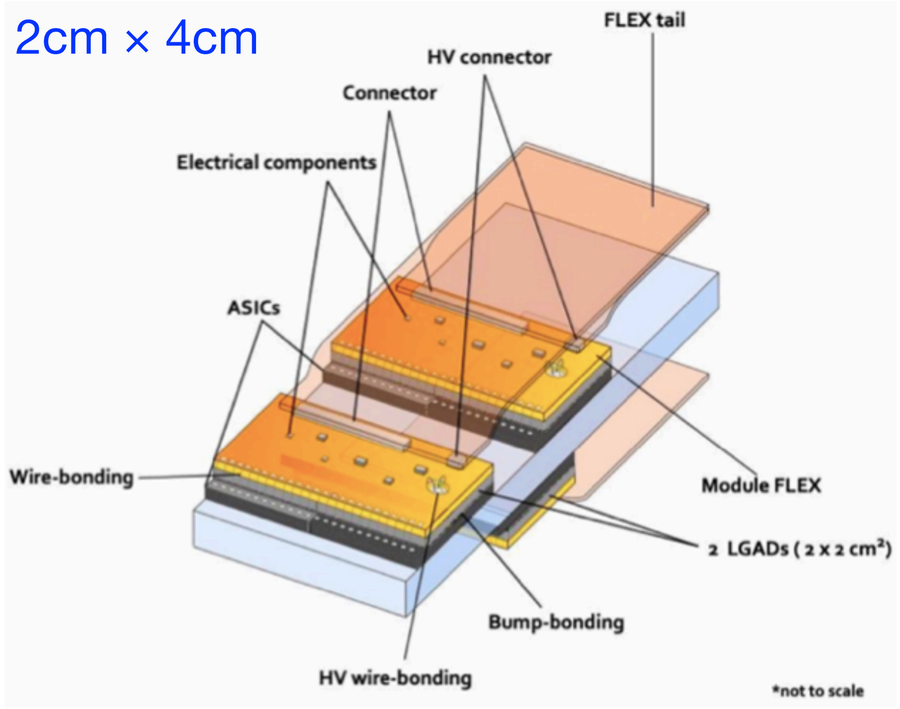

Radiation environment

HGTD Public Results

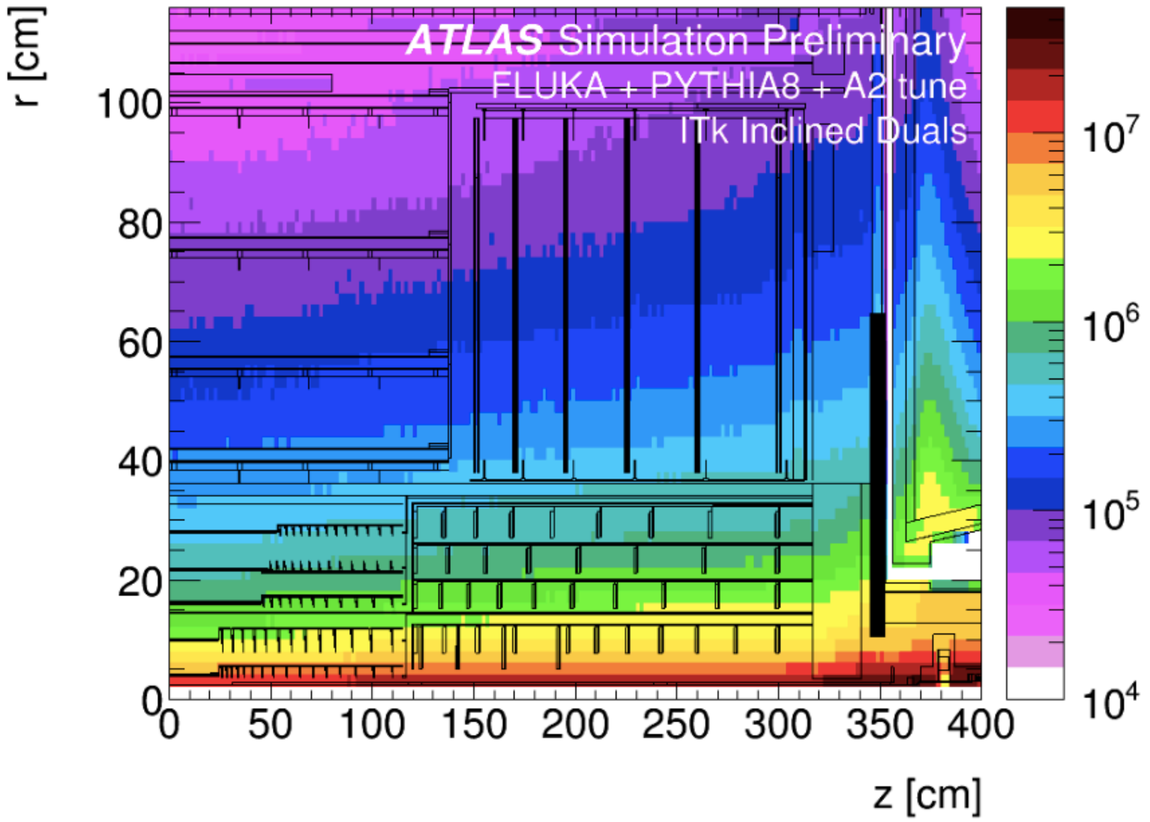

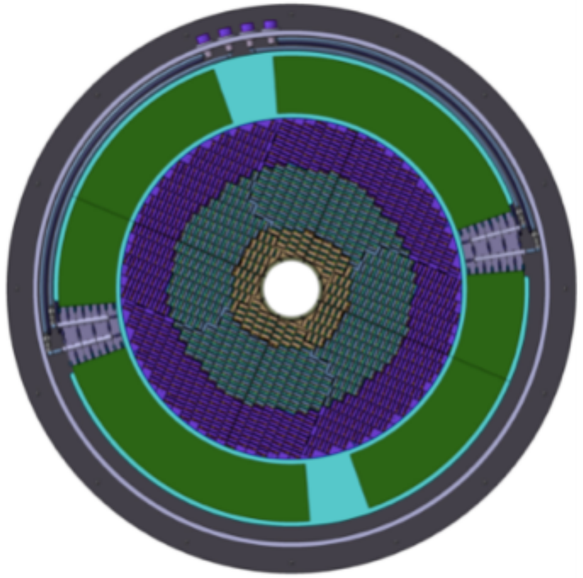

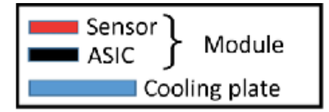

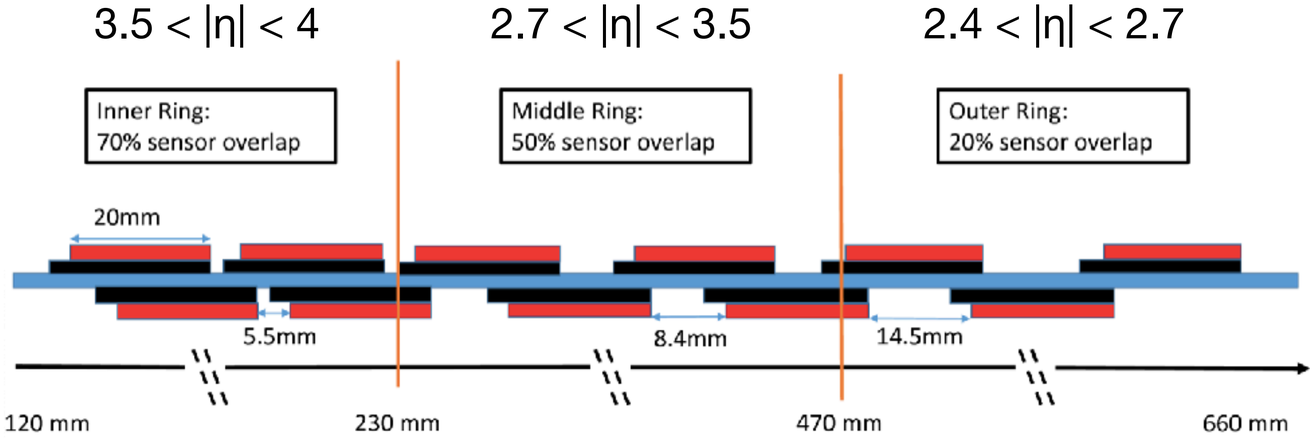

Max neutron fluence/dose after 4000 fb^{-1}:

2.5x10^{15} n_{eq}/cm^2 and 2 MGy

Replaced every 1000 fb^{-1} Replaced every 2000 fb^{-1} 4000 fb^{-1}

Radiation environment - impact on physics performance

HGTD Public Results

Track time resolution as function of integrated luminosity

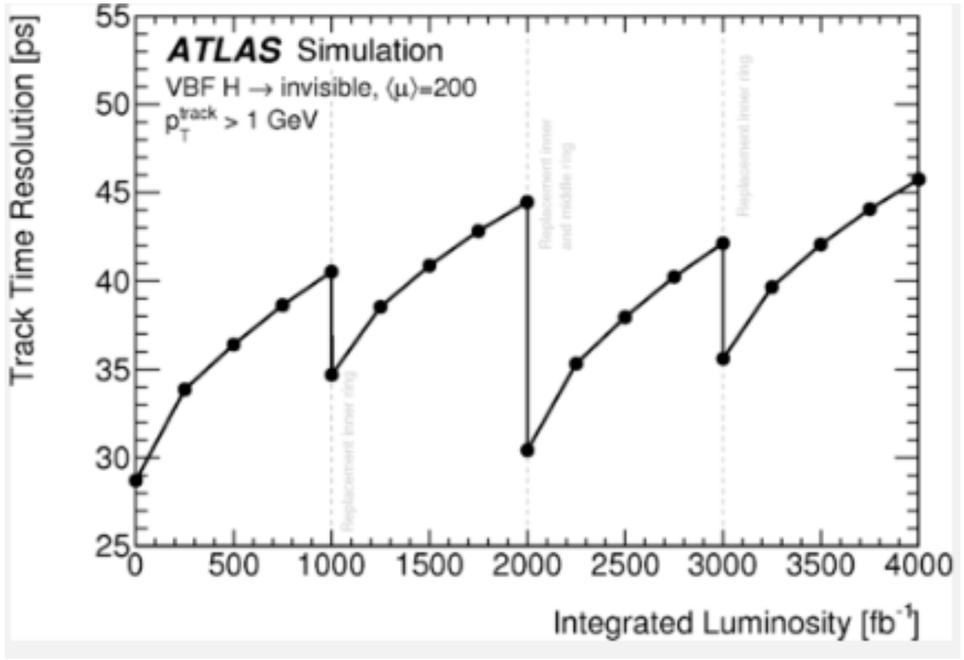

Inner and middle rings have to be replaced to maintain the target timing resolution. After the replacement the performance is (partially) recovered.

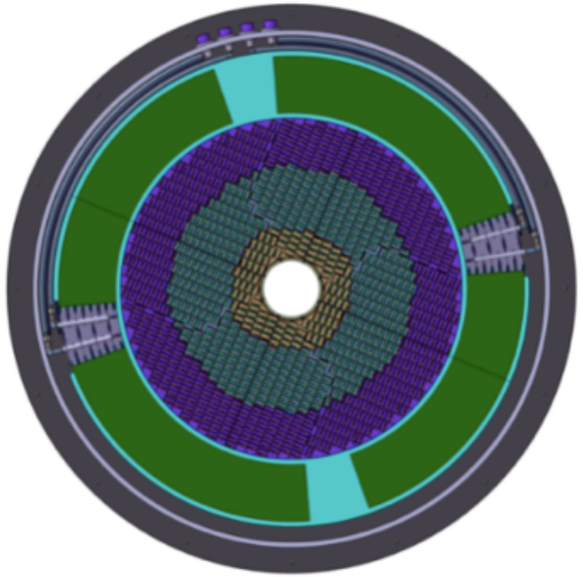

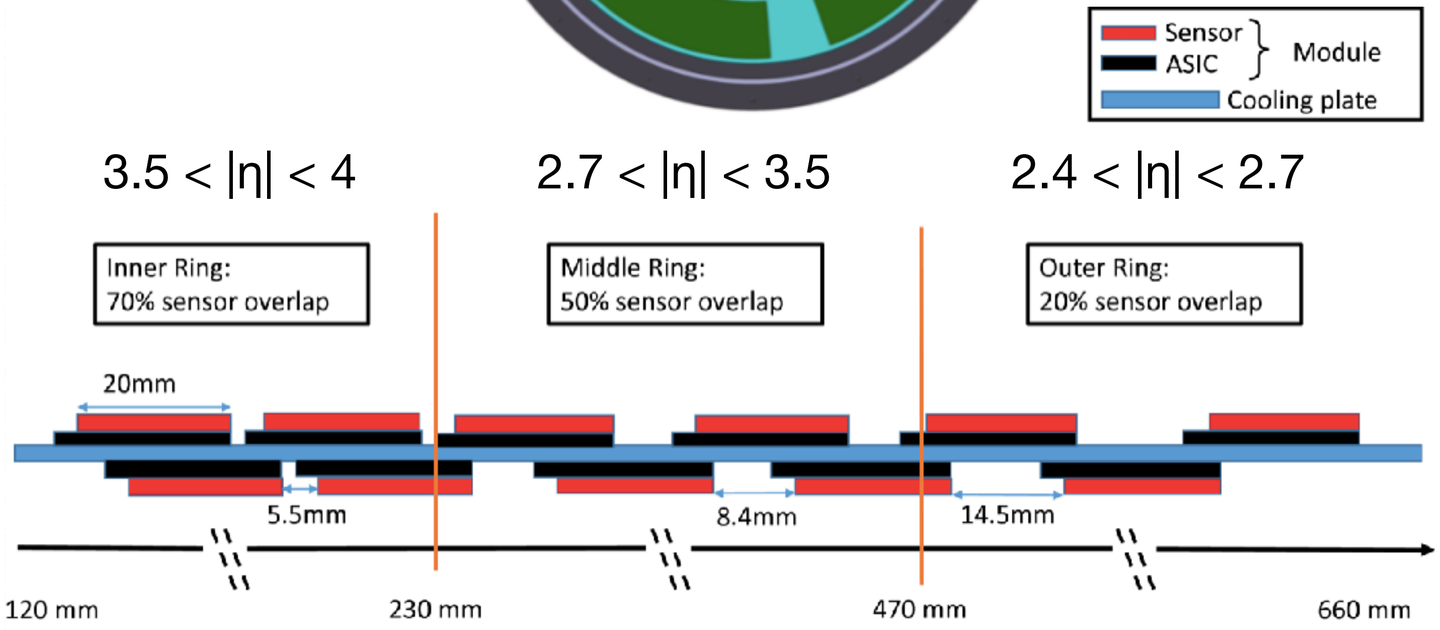

Replaced every 1000 fb^{-1} Replaced every 2000 fb^{-1} 4000 fb^{-1}

R&D for an hybrid detector

An HGTD module is a hybrid silicon detector with an LGAD bump-bonded to an ASIC

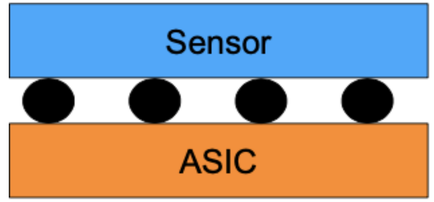

Thickness of LGADs is crucial to mitigate the jitter

Tested LGADs down to ~ 35 μm active Si

- Smaller rise time —> faster signal —> less impact due to Landau fluctuations
- Lower bias voltages reduce power dissipation —> less cooling requirements
- Thin LGADs have relatively large capacitance, around 4 pF for 50 µm thickness.

$$\sigma_{\text{jitter}} = \frac{e_n C_d \sqrt{t_d}}{Q_{\text{inj}}}$$

Jitter of a preamplifier:

e_n [V/√Hz]: voltage noise spectral density

C_d: detector capacitance seen by the front-end

t_d: rise time

Q_{inj}: signal charge

Multiplication layer design

- Gain is constrained by noise (< 100)
- p-gain layer depth (up to 2.5 μm)
- Materials
- Doping profile

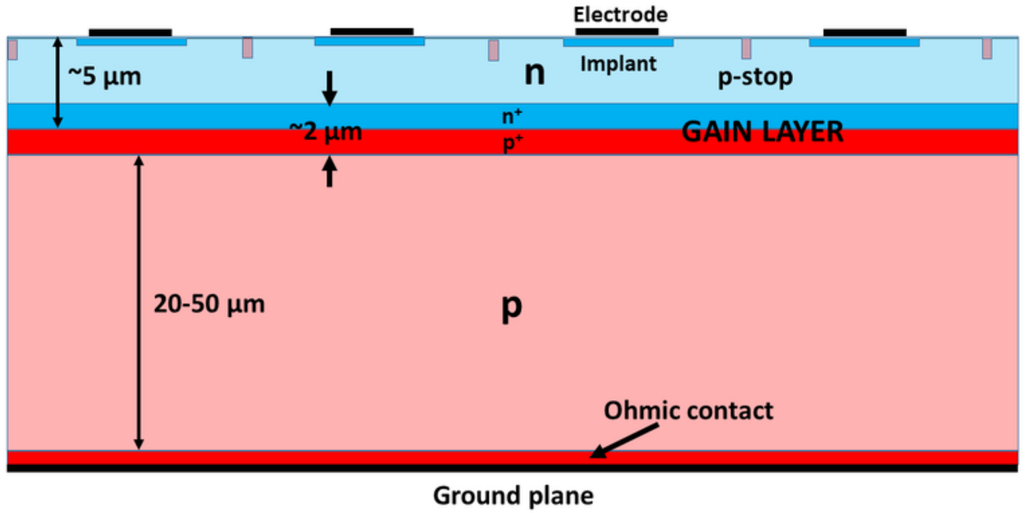

Hybridisation

S. Grinstein - Tredi 2025

Bump-Bonding of LGAD Sensors to the ALTIROC ASIC

- Similar to pixel detector but less demanding due to larger pads
- Under-bump metallisation of both ASIC and sensor
- Solder bump deposition on ASIC

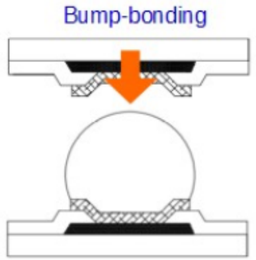

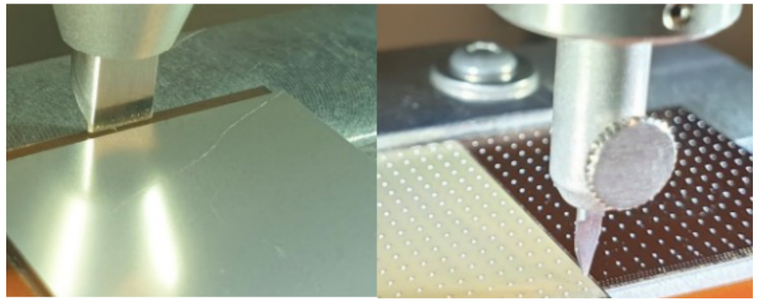

Tests

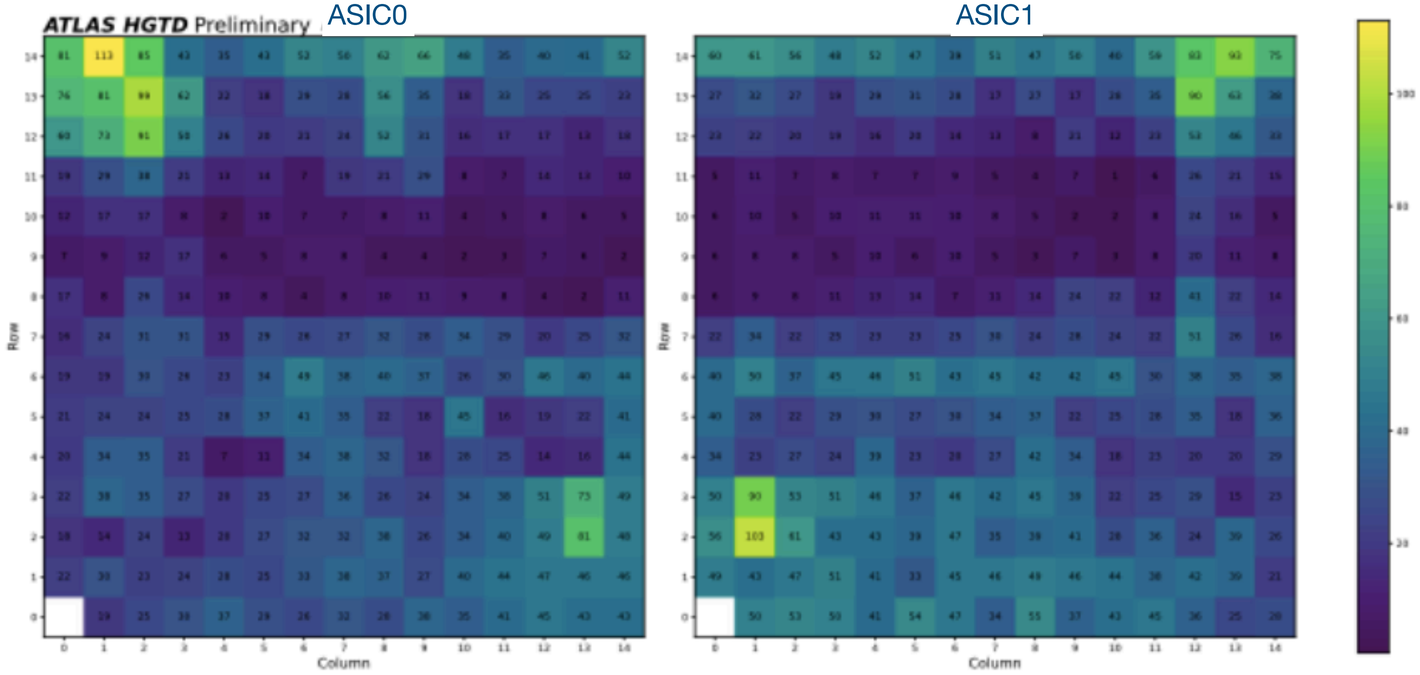

Check for disconnected bumps with a 90Sr source. Scan of two ASICs after 120 thermal cycles.
Pixel (0,0) is left disconnected for reference.

Compare front-end discriminator thresholds with different injected charges

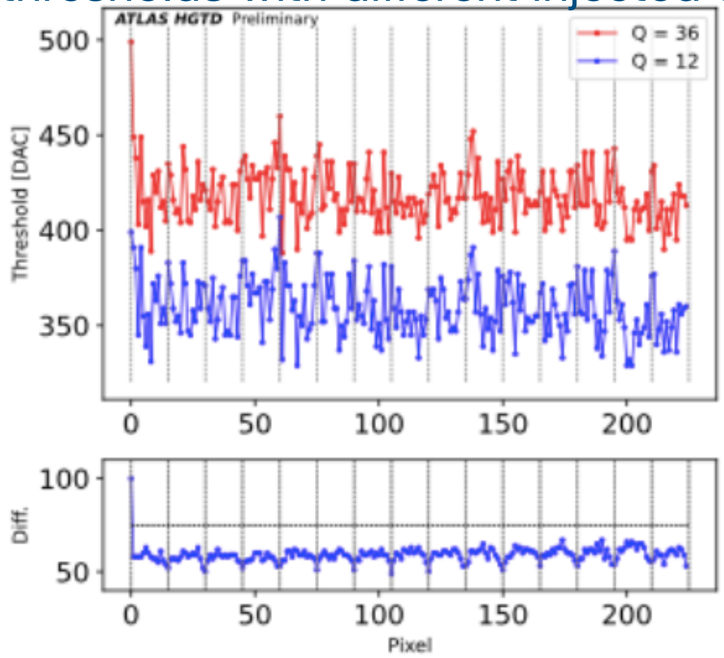

Consistent separation between the two curves
—> uniform and linear front-end response

Radiation hardness R&D - acceptor removal

HGTD Public Results

Irradiation above fluences of 1.5x10^{15} n_{eq}/cm^2 significantly rlower the effective doping in the p-gain layer reducing the electric field —> internal gain drops

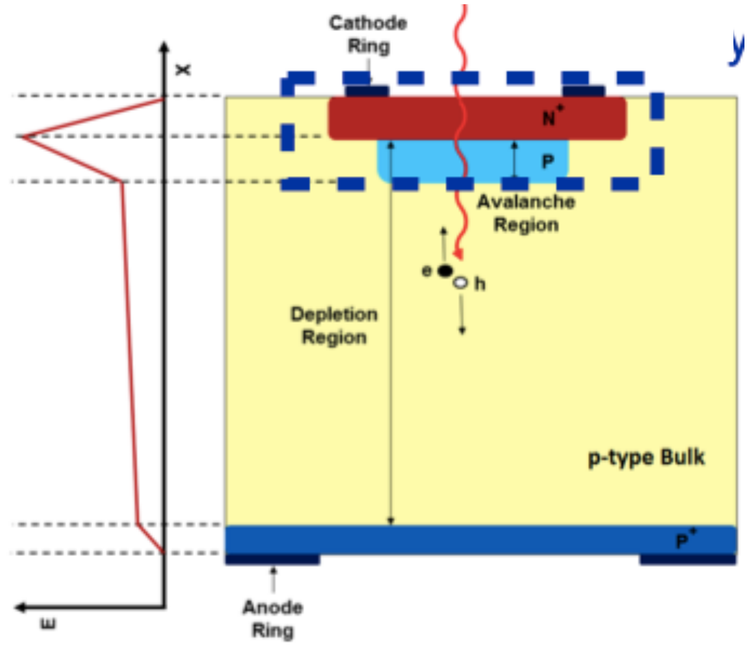

Studies of different gain layer designs and doping materials

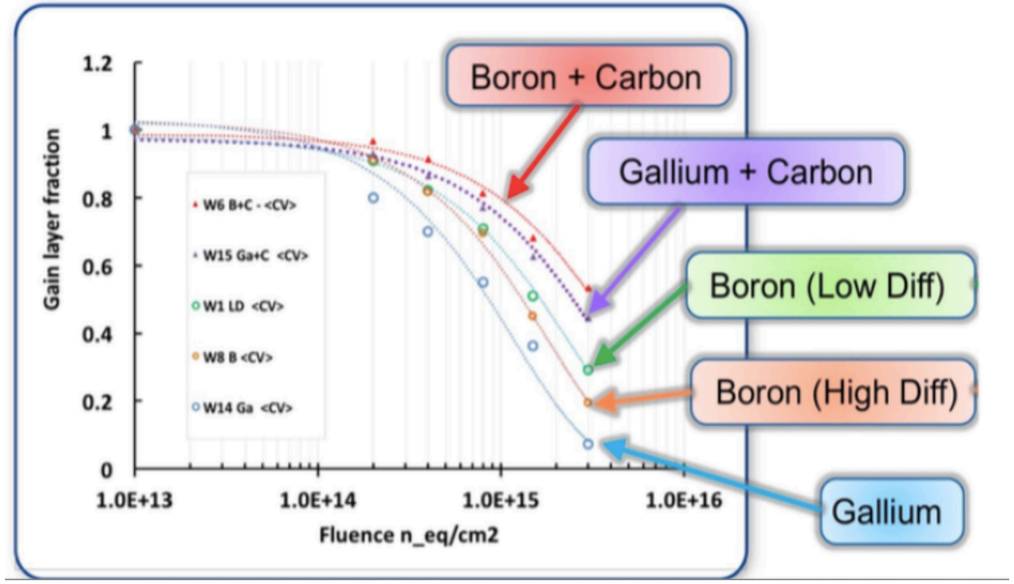

Least loss in gain from carbon-enriched substrates boron + carbon preserve the doping better

Radiation hardness R&D - the unexpected

JINST 17 (2022) C07020

Testbeam campaigns revealed LGAD failures consistent with single-event burnout, a mechanism well known in high-voltage power semiconductors but never observed in **thin silicon timing detectors**

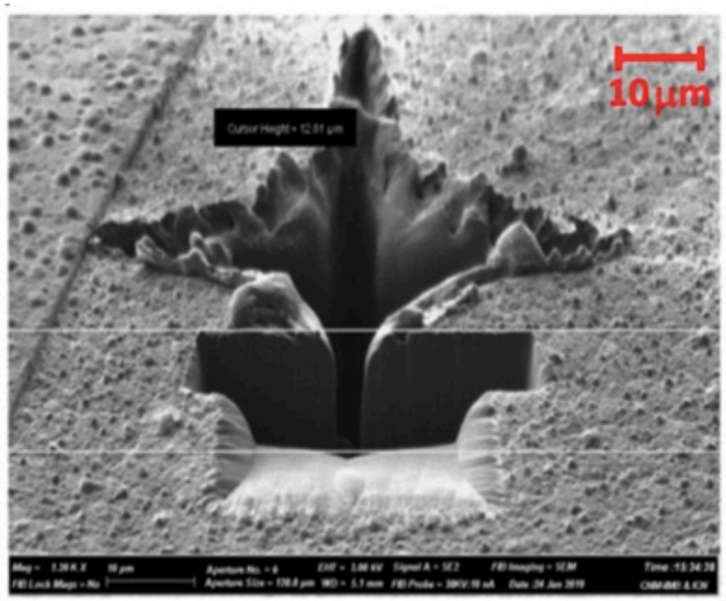

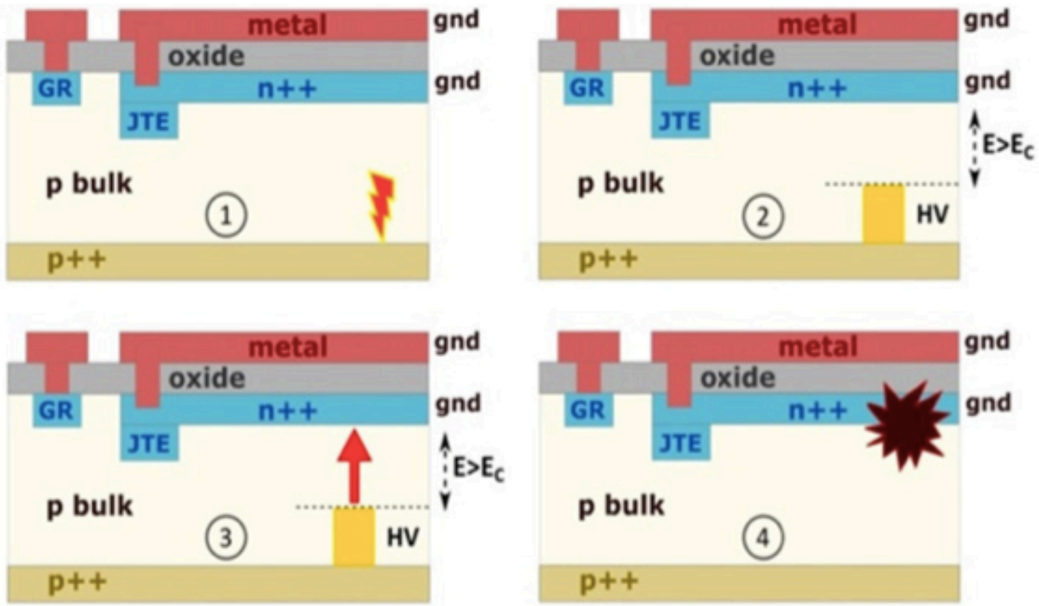

1 - Large, localised charge deposition

2 - Field collapse due to high carrier density

3 - This pulls HV closer to the pad → huge field

4 - Irreversible avalanche breakdown and permanent damage

This established SEB as a fundamental operational constraint for irradiated LGADs at high bias voltage

Establishing the safe operating conditions

2023 JINST 18 P07030

- Test campaigns were conducted at DESY and required collaboration with vendors, RD50, and CMS ETL (EndCap Timing Layer)

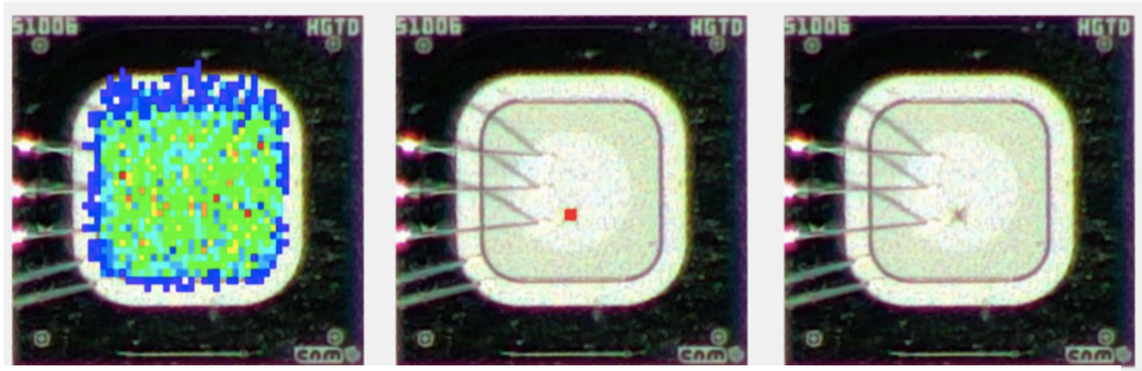

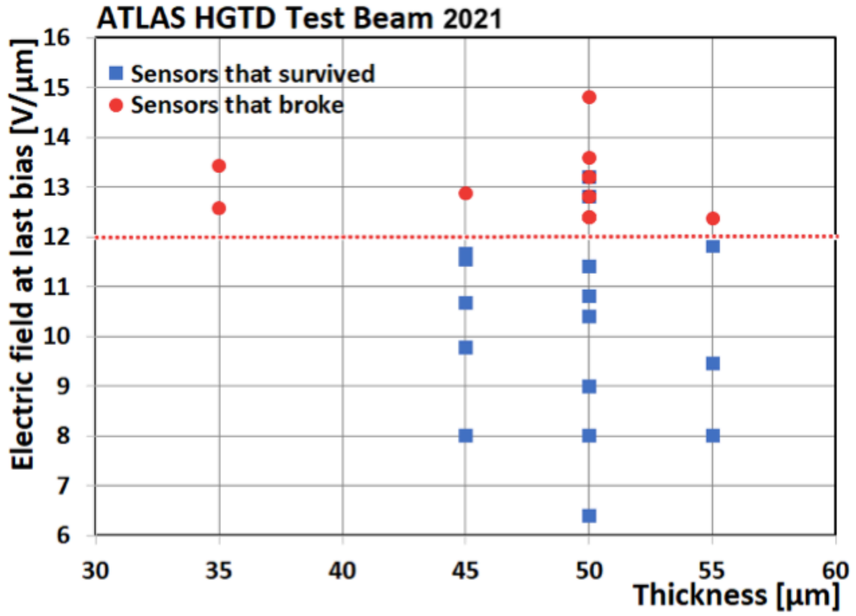

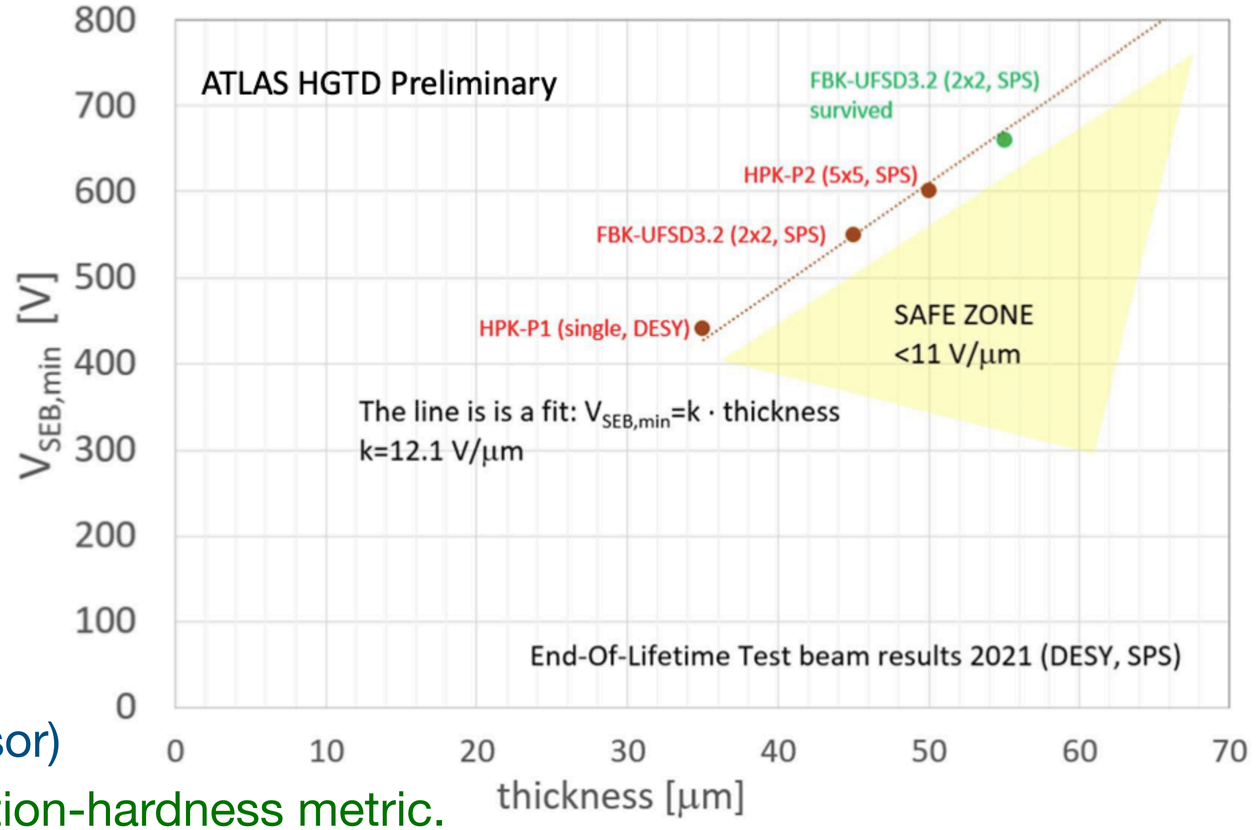

$V_{op} < 11$ V/μm

Operating condition: Voltage < 550 V (for a 50 µm sensor)

In practice this condition is never reached. It is a radiation-hardness metric.

Radiation hardness R&D - acceptor removal (II)

HGTD Public Results

We have seen that radiation induces acceptor removal in the p-gain layer, reducing the electric field and leading to loss of gain

→ Study gain layer depletion voltage, V_{gl}, dependence on fluence: $V_{gl} = V_{gl,0} \times e^{-c\Phi_{eq}}$

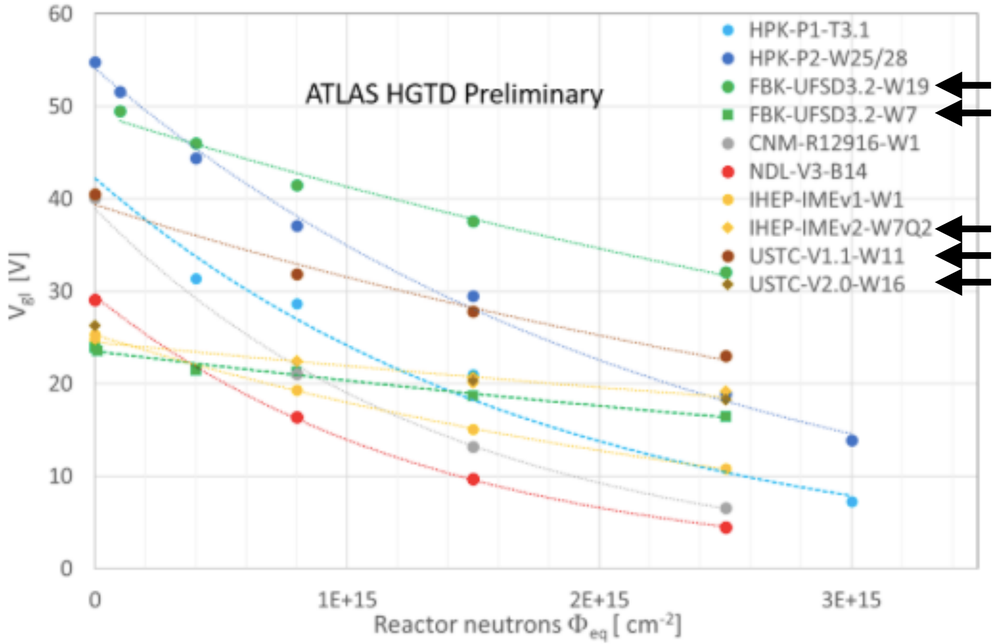

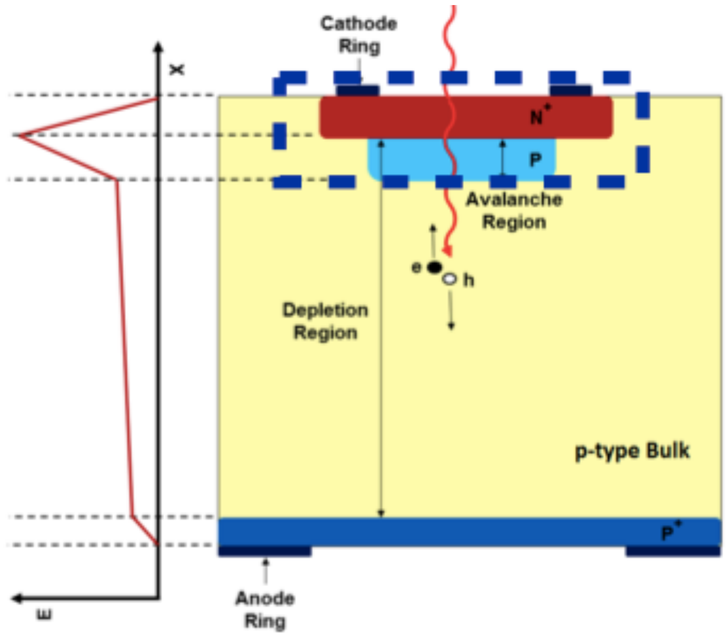

From C-V measurements: lowest acceptor removal with carbon-enriched wafers

Radiation hardness R&D - acceptor removal (II)

We have seen that radiation induces acceptor removal in the p-gain layer, reducing the electric field and leading to loss of gain

→ Study p-gain layer depletion voltage, V_{gl}, dependence on fluence: $V_{gl} = V_{gl,0} \times e^{-c\Phi_{eq}}$

Recover by increasing the bias

- Limit imposed by p-gain layer voltage breakdown (and by single-event burnout (SEB)

→ V_{max}~550 V for 50 µm thickness)

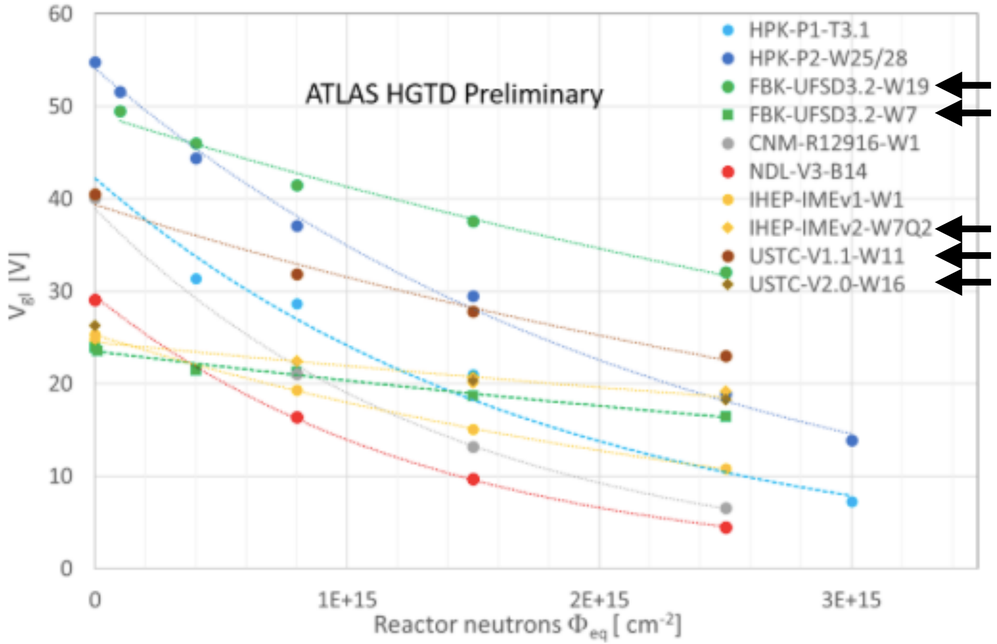

From C-V measurements: lowest acceptor removal with carbon-enriched wafers

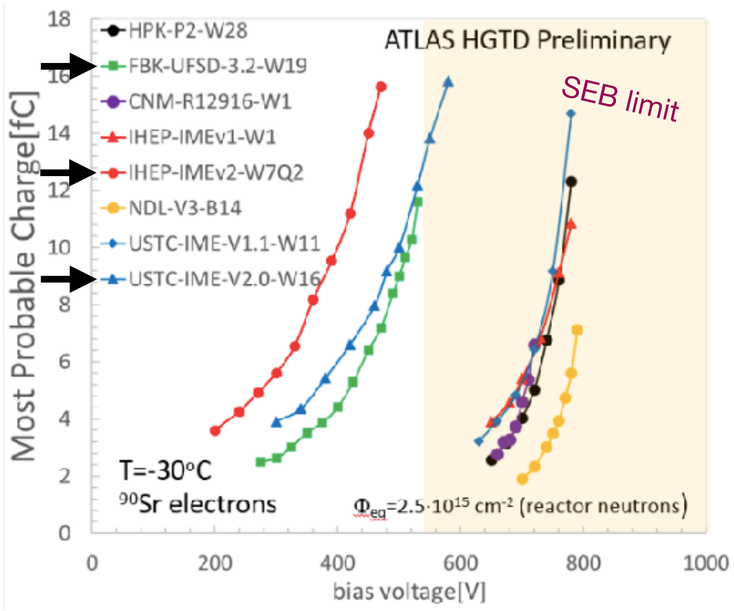

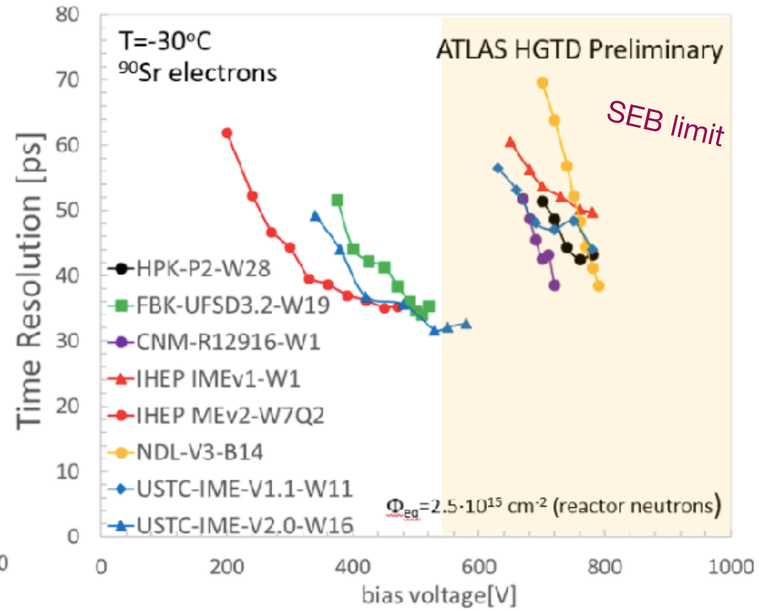

FBK-UFSC-2.3-W19, IHEP-IMEv2-W7Q2, USTC-IME-V2.0-W16 sensors show stable performance at much lower bias voltages than non-carbon enriched wafers

Irradiation tests - TCT measurements

NIMA 1084 (2026) 171195

Transition Current Technique - performed in the interface region of two LGAD devices

- p-gain layer depletion voltage (V_{gl}) extraction
- Gain dependence on bias voltage
- Sensor leakage current
- Effective interpad distance

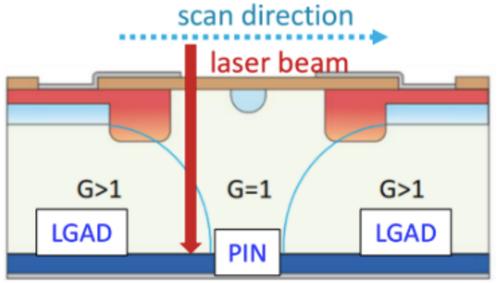

Vendor: IHEP-IME

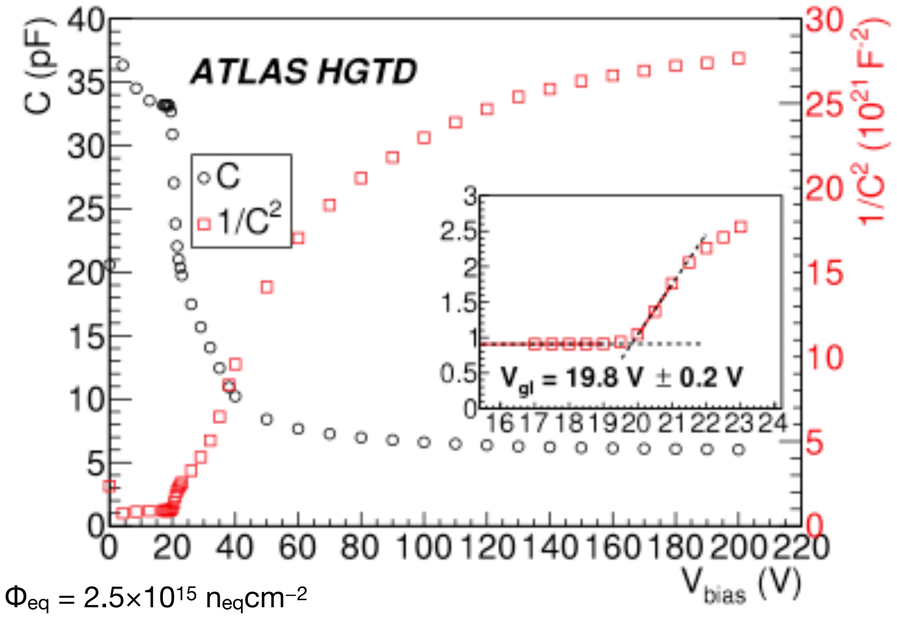

$\Phi_{eq} = 2.5\times10^{15}$ $n_{eq}cm^{-2}$

Inset shows V_{gl} extraction from the intersection of two linear fits

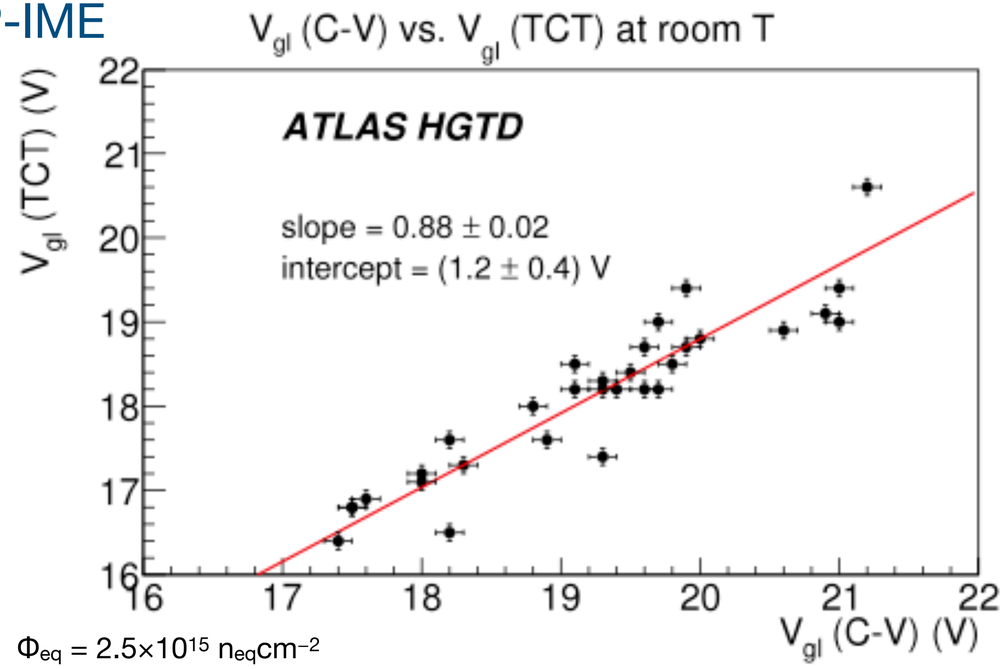

$\Phi_{eq} = 2.5\times10^{15}$ $n_{eq}cm^{-2}$

Systematic offset between V_{gl} from TCT and C–V measurements
→charge-collection vs capacitance/depletion

Association of HGTD timing measurement to a track

HGTD Public Results

- HGTD provides hit timestamps $t_{hit,i}$ for each associated cluster
- ITk tracks are extrapolated to HGTD layer-by-layer using a progressive Kalman filter
- In each HGTD layer, hits near the extrapolated track position are tested and the lowest-χ^2 hit is selected as the track extension.
- **Track time**: average of the TOF-corrected times of the associated hits

$$t_{track} = \frac{1}{N}\Sigma_i(t_{hit,i} - TOF_i)$$

Association of HGTD timing measurement to a track

HGTD Public Results

- HGTD provides hit timestamps $t_{hit,i}$ for each associated cluster
- ITk tracks are extrapolated to HGTD layer-by-layer using a progressive Kalman filter
- In each HGTD layer, hits near the extrapolated track position are tested and the lowest-χ^2 hit is selected as the track extension.
- **Track time**: average of calibrated TOF-corrected times of all HGTD hits associated to the track

$$t_{track} = \frac{1}{N}\Sigma_i(t_{hit,i} - TOF_i)$$

track-to-vertex time association

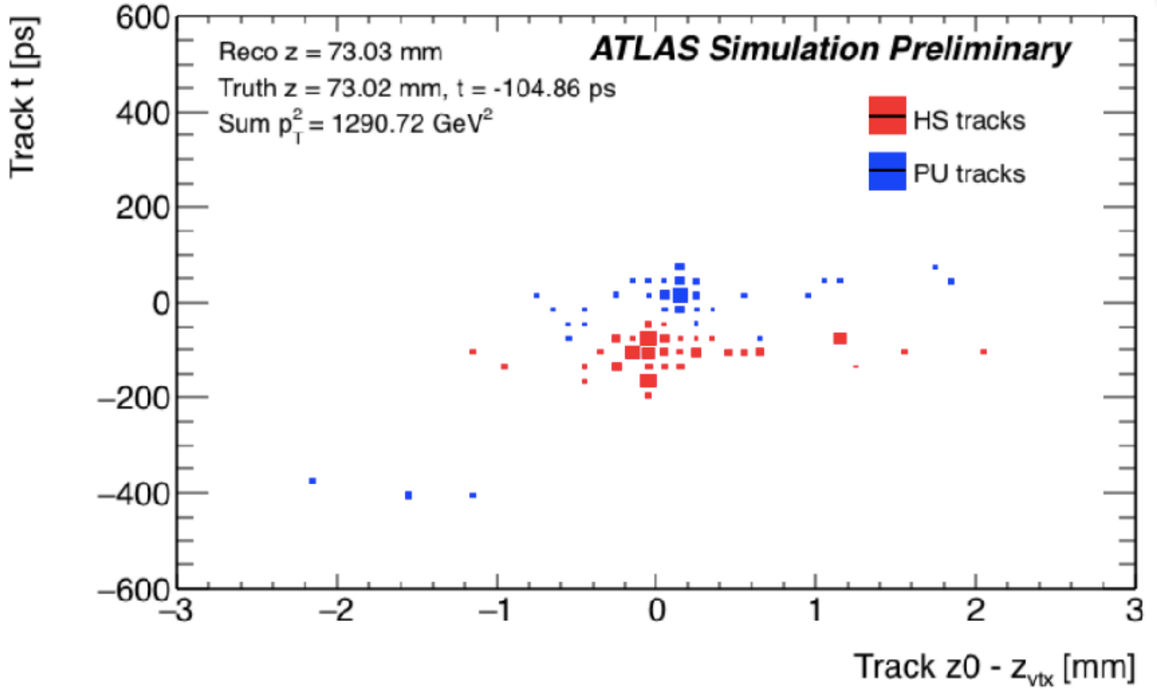

tracks from the same vertex should cluster in time

tracks from different vertices often differ by tens to hundreds of ps

Time measurement in LGAD readout: TOA and Vernier TDC

Time of Arrival (TOA) of a particle**,** relatively to its bunch-crossing (BC) ID, is measured in a 2.5 ns time window, centred on the expected arrival time of particles from that BC

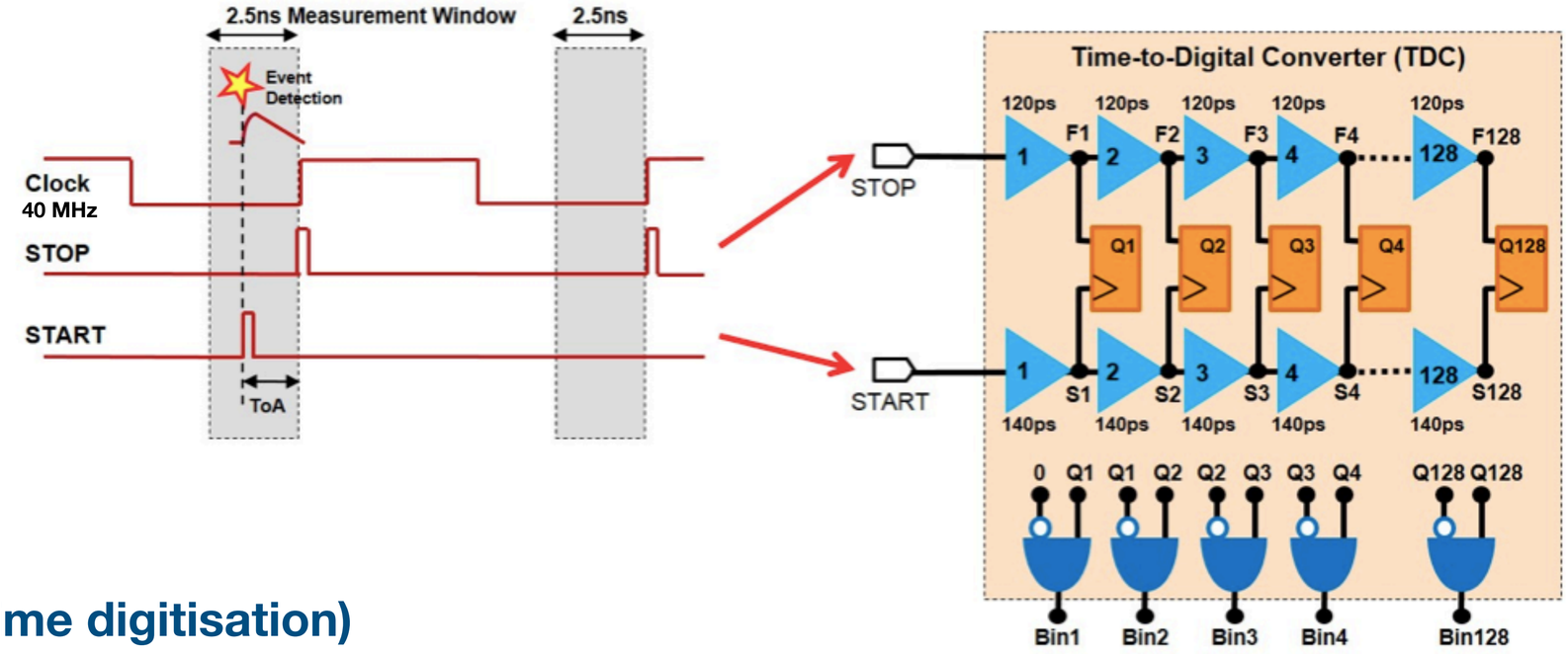

Vernier TDC (fine time digitisation)

- Two lines with slightly different delays (“Vernier lines”), each composed of a series of delay cells
- Control voltages set each cell delay to 140 ps (slow line) and 120 ps (fast line)
- With START initially ahead of STOP, each stage reduces their time difference by LSB = $\Delta t = 140 - 120 = 20$ ps
- The TOA is quantised and determined by the first bin where STOP overtakes START
- Example: for a physical TOA = 50 ps, the TDC selects Bin3 and therefore TOA $\in$ [40ps, 60ps)

Time Measurement in LGAD Readout: TOA, TOT and Vernier TDC

HGTD Public Results

- Timing and hit data stored in local registers
- On Level0 Accept they are sent off-chip (≤ 35 μs latency)
- Luminosity derived from hit rate per ASIC per bunch-crossing

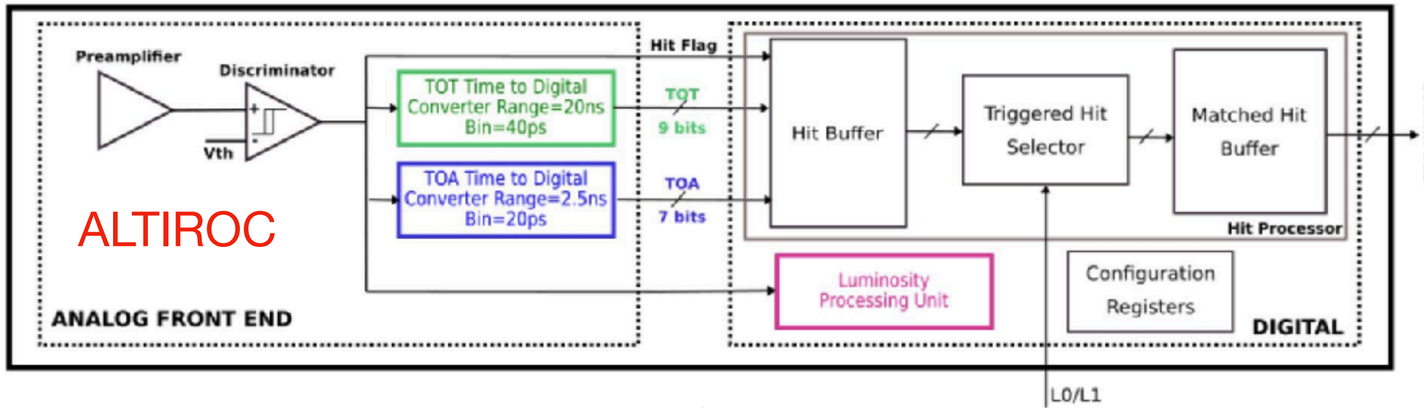

TOA TDC calibration: Vernier delay lines (120 ps / 140 ps per stage)

Control-voltage difference required to achieve a given TOA bin width (LSB)

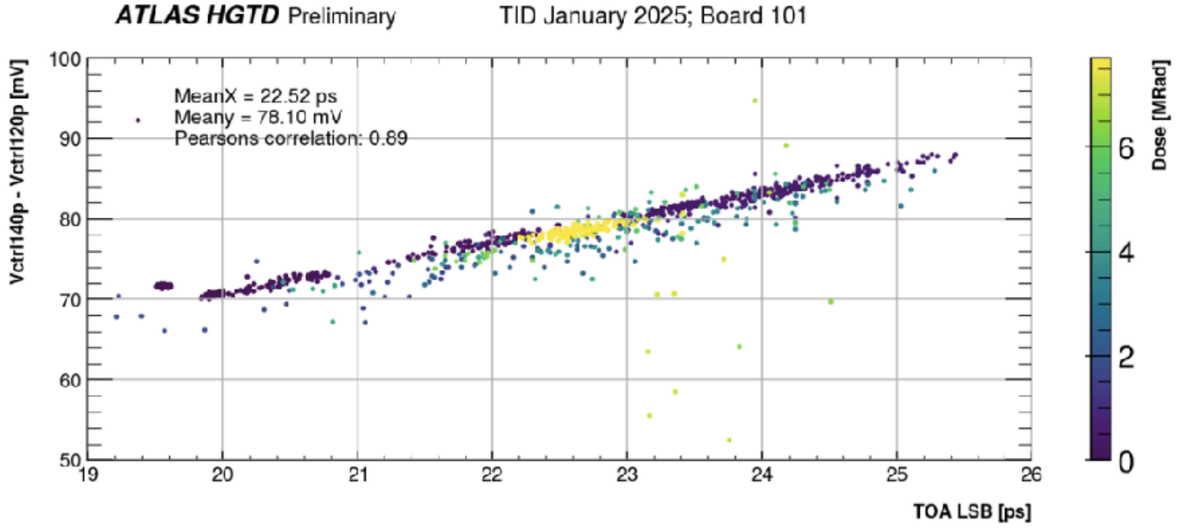

Larger V_{ctrl} difference → wider time bin (lower TDC resolution)

Stable correlation under irradiation

Time Measurement in LGAD Readout: TOA, TOT and Vernier TDC

HGTD Public Results

- Timing and hit data stored in local registers
- On Level0 Accept they are sent off-chip (≤ 35 μs latency)
- Luminosity derived from hit rate per ASIC per bunch-crossing

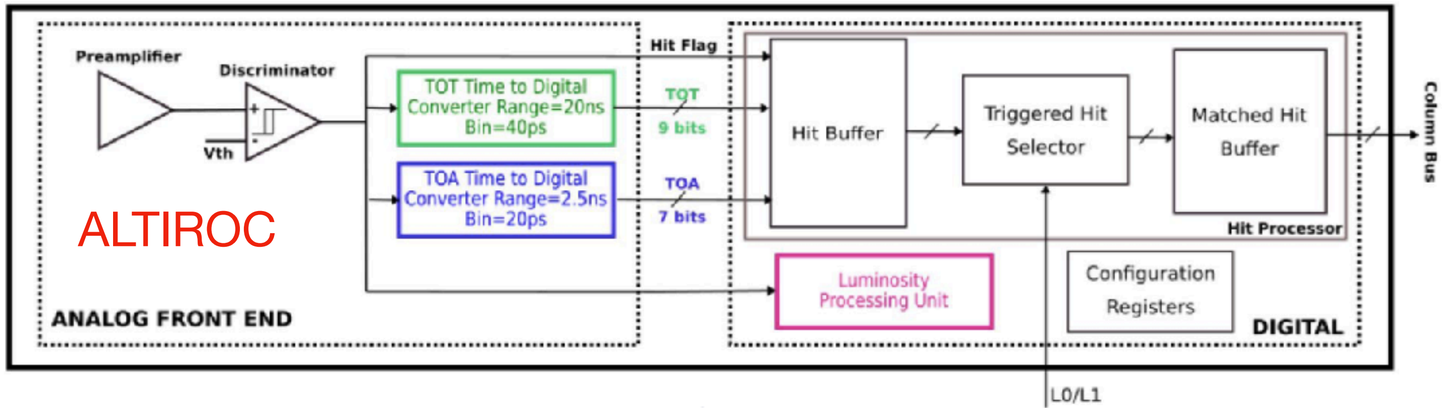

TOA TDC calibration: Vernier delay lines (120 ps / 140 ps per stage)

Control-voltage difference required to achieve a given TOA bin width (LSB)

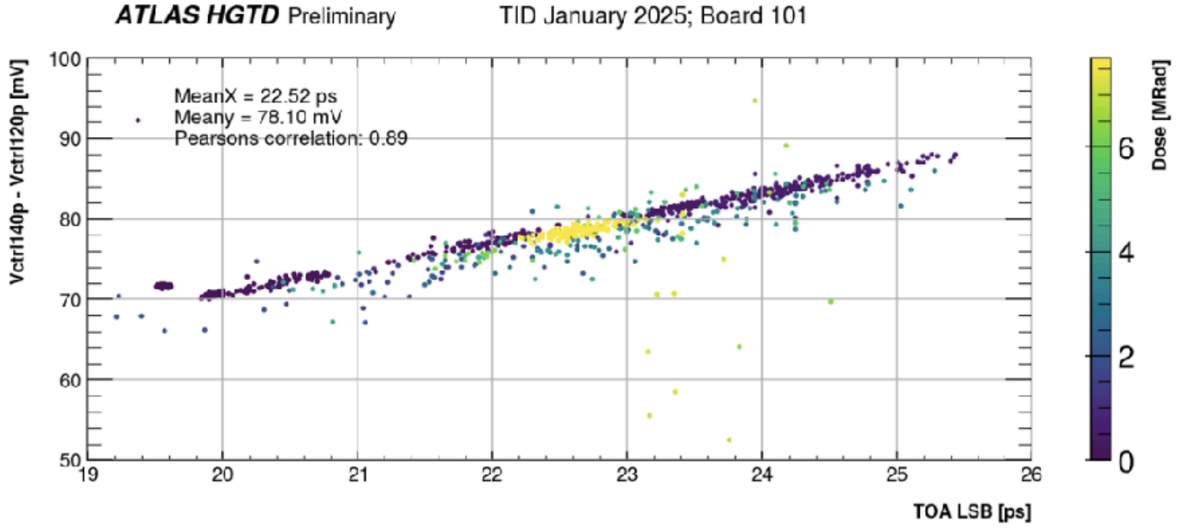

Larger V_{ctrl} difference → wider time bin (lower TDC resolution)

Stable correlation under irradiation

TOT (Time-over Threshold):
used to correct TOA shifts due to time-walk

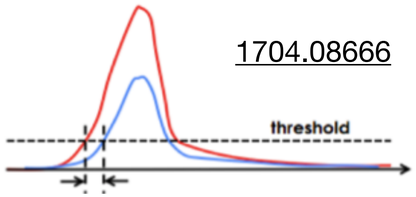

TOA before and after TOT-based time-walk correction

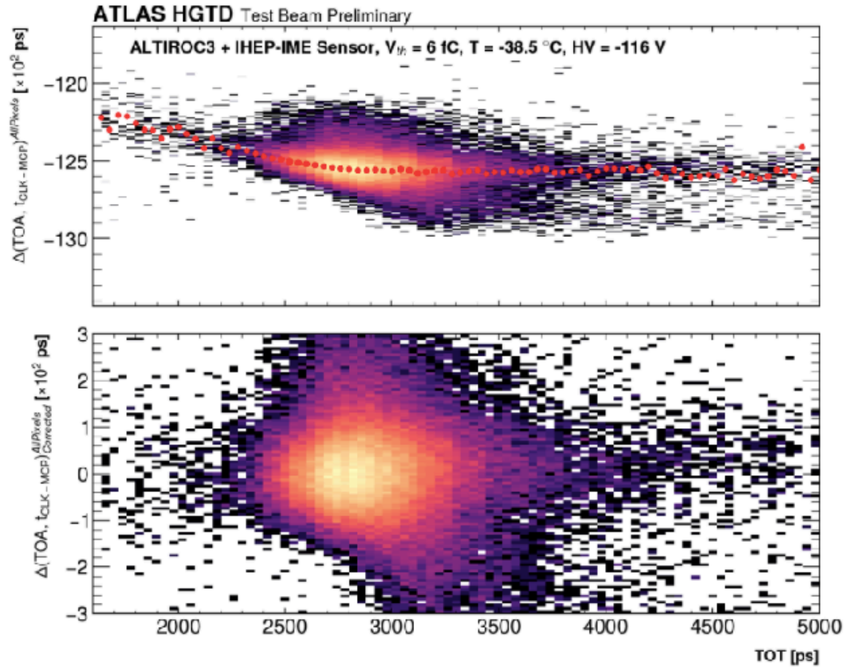

After correction TOA residuals are flat

Time Resolution

$$\sigma^2_{total} = \sigma^2_{Landau} + \sigma^2_{jitter} + \sigma^2_{TimeWalk} + \sigma^2_{TDC} + \sigma^2_{clock}$$

sensor

σ^2_{Landau}: Landau fluctuations from deposited energy as charged particle traverses the sensor

N. Cartiglia, PSD12

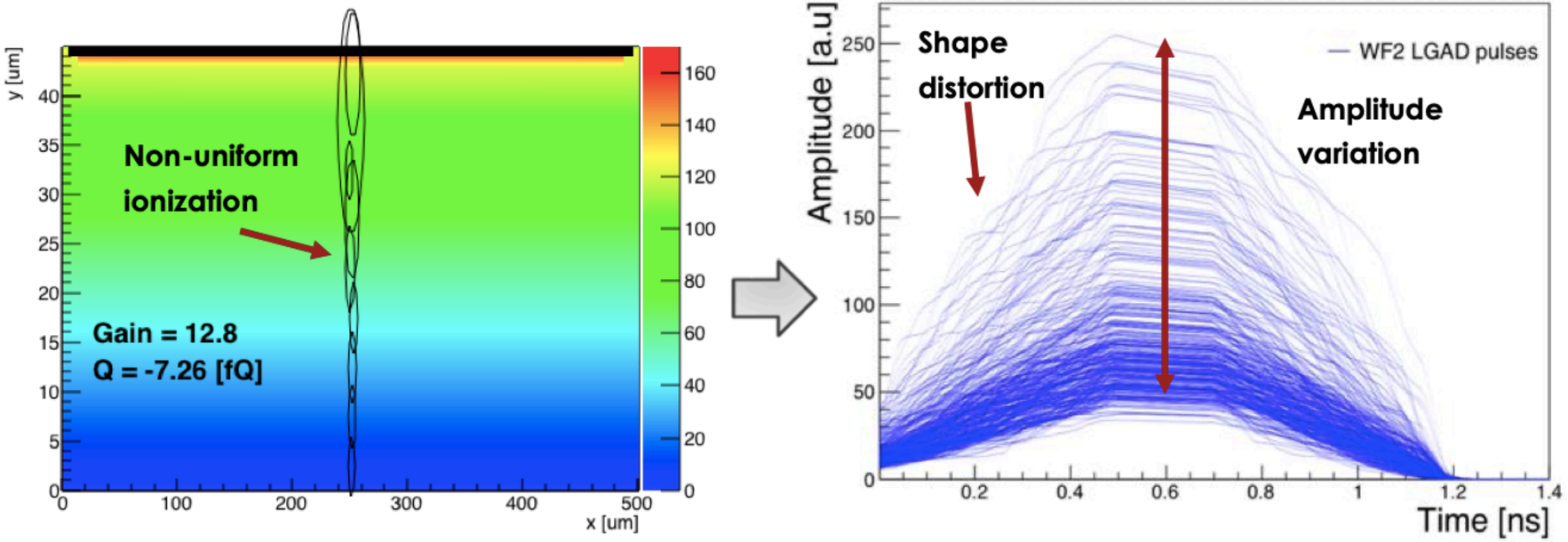

These variations are not noise; They come from different ionisation patterns inside the silicon

Time resolution is ultimately limited by non-uniform ionisation

< 25 ps pre-irradiation: thin sensors

Time Resolution

N. Cartiglia et al. 1704.08666

sensor + ASIC

$$\sigma^2_{total} = \sigma^2_{Landau} + \sigma^2_{jitter} + \sigma^2_{TimeWalk} + \sigma^2_{TDC} + \sigma^2_{clock}$$

- **Preamplifier:** Amplifies and shapes the sensor signal
- **Comparator:** Receives the pulse and defines the time of arrival
- **Time Definition:** The moment the pulse crosses a fixed discriminator threshold (V_{th})

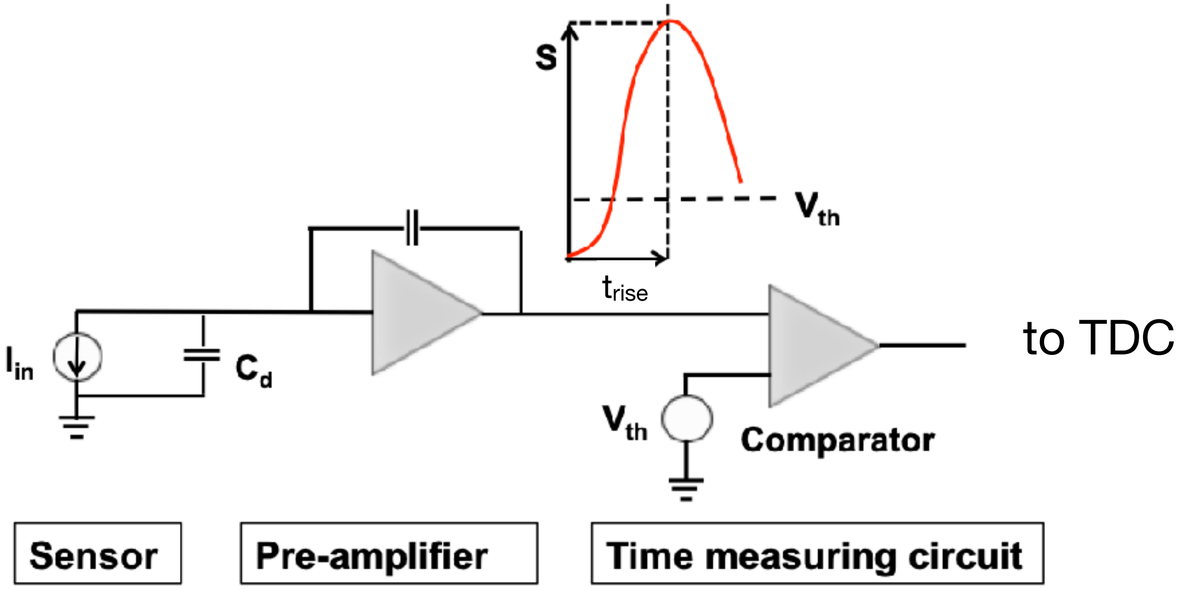

This threshold-crossing method introduces electronic jitter and TimeWalk

Time Resolution

N. Cartiglia et al. 1704.08666

sensor + ASIC

$$\sigma^2_{total} = \sigma^2_{Landau} + \sigma^2_{jitter} + \sigma^2_{TimeWalk} + \sigma^2_{TDC} + \sigma^2_{clock}$$

$$\sigma_{jitter} = \frac{N}{dV/dt} \approx t_{rise}/\frac{S}{N}$$

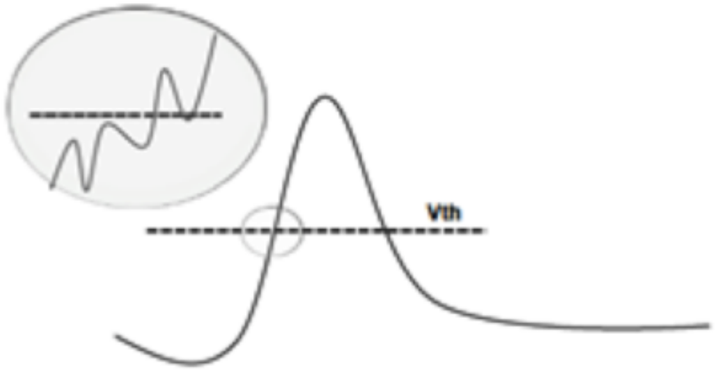

The jitter term is the time uncertainty induced by electronic noise when the signal crosses the threshold V_{th}.

Time Resolution

N. Cartiglia et al. 1704.08666

sensor + ASIC

$$\sigma^2_{total} = \sigma^2_{Landau} + \sigma^2_{jitter} + \sigma^2_{TimeWalk} + \sigma^2_{TDC} + \sigma^2_{clock}$$

$$\sigma_{jitter} = \frac{N}{dV/dt} \approx t_{rise}/\frac{S}{N}$$

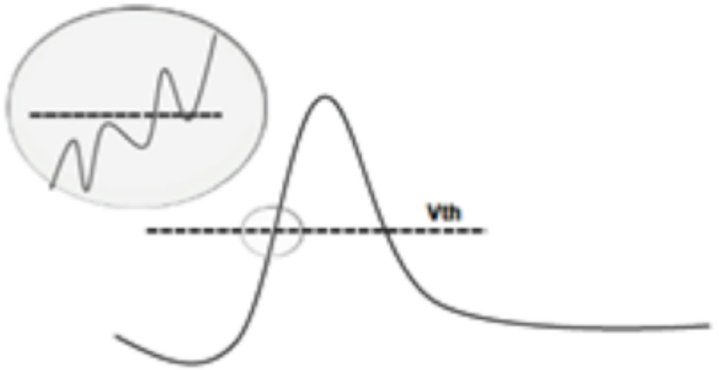

The jitter term is the time uncertainty induced by electronic noise when the signal crosses the threshold V_{th}.

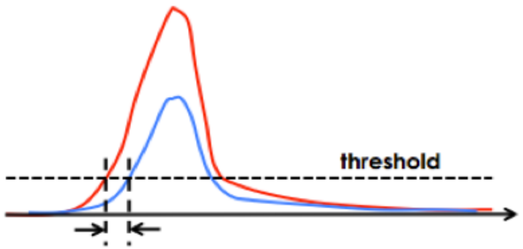

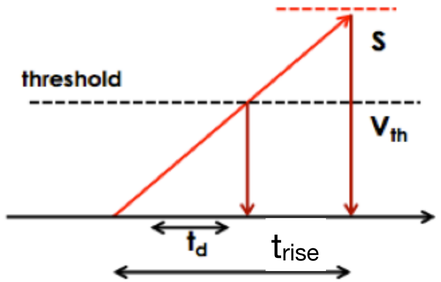

$$\sigma_{TimeWalk} = [t_d]_{RMS} = [\frac{V_{th}}{S/t_{rise}}]_{RMS}$$

TimeWalk: signals of different amplitudes cross a fixed threshold at different times, generating an amplitude-dependent delay t_d when firing the discriminator. This is also an unavoidable effect.

Time Resolution - results

HGTD Public Results

ASIC + readout

$$\sigma^2_{total} = \sigma^2_{Landau} + \sigma^2_{jitter} + \sigma^2_{TimeWalk} + \sigma^2_{TDC} + \sigma^2_{clock}$$

- TOA calibration applied here includes:

  - Per-channel TOA linearisation, performed using either internal charge injection (ASIC)

Charge injection, no TWC

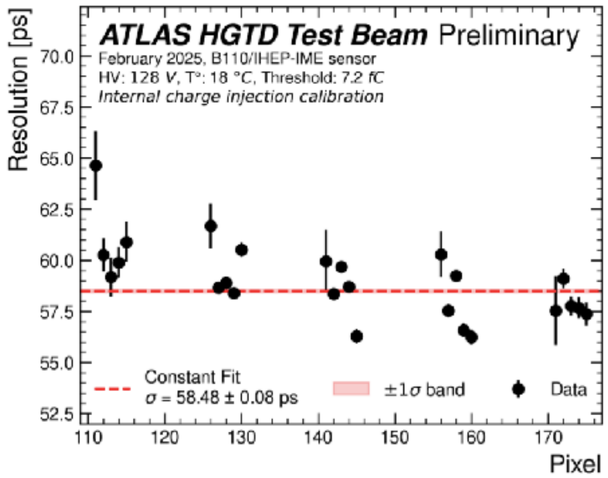

Time Resolution - results

HGTD Public Results

$$\sigma^2_{total} = \sigma^2_{Landau} + \sigma^2_{jitter} + \sigma^2_{TimeWalk} + \sigma^2_{TDC} + \sigma^2_{clock}$$

ASIC + readout

- TOA calibration applied here includes:
  - Per-channel TOA linearisation, performed using either internal charge injection (ASIC) or testbeam data (with LGAD signals)
    - With and without TOT-based time-walk correction

Charge injection, no TWC

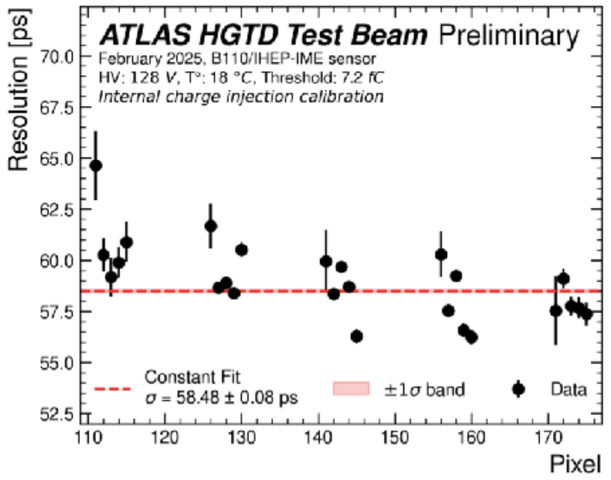

TB data, no TWC

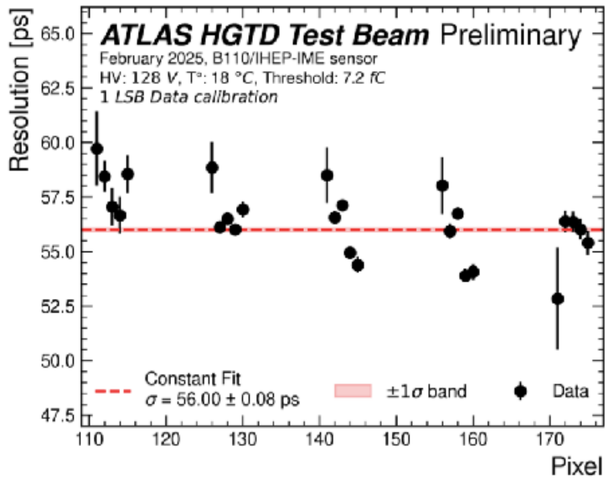

TB data, with TWC

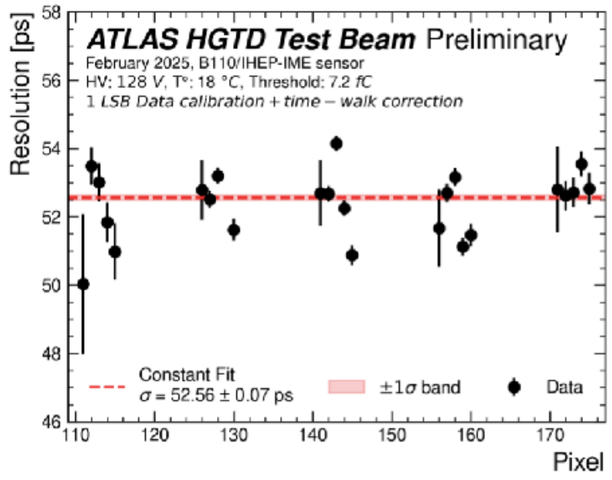

TB data, 4 LSB corr. for DNL, with TWC

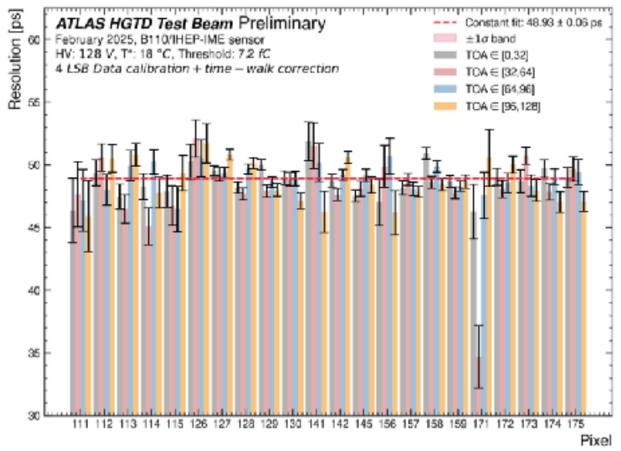

On the right, events are split into four fine-TOA (TDC) code regions to check whether the timing resolution depends on where the hit falls inside the TDC measurement window.

Data-driven method improves resolution significantly (down to ~49 ps), **exposing the intrinsic sensor limit**

Time Resolution - results

HGTD Public Results

$$\sigma^2_{total} = \sigma^2_{Landau} + \sigma^2_{jitter} + \sigma^2_{TimeWalk} + \sigma^2_{TDC} + \sigma^2_{clock}$$

ASIC + readout

Performance of ALTIROC in optimal operating conditions:

– Low temperature (–35 °C), high bias (>120 V), low threshold (4 fC)

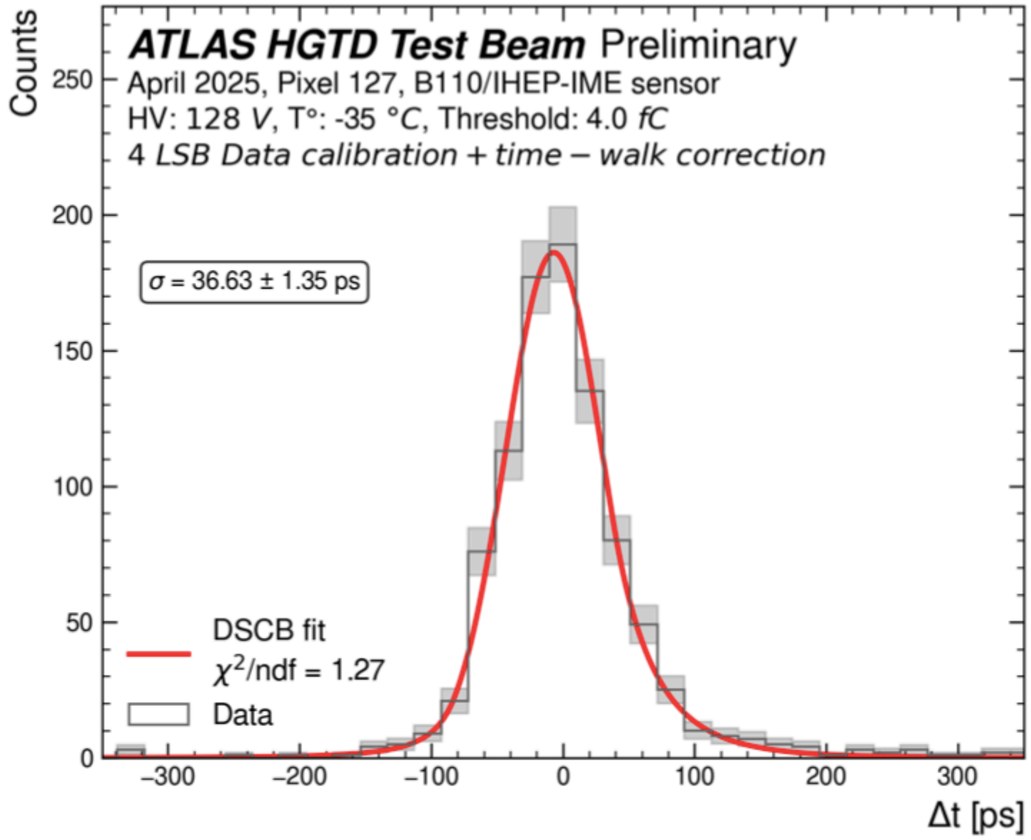

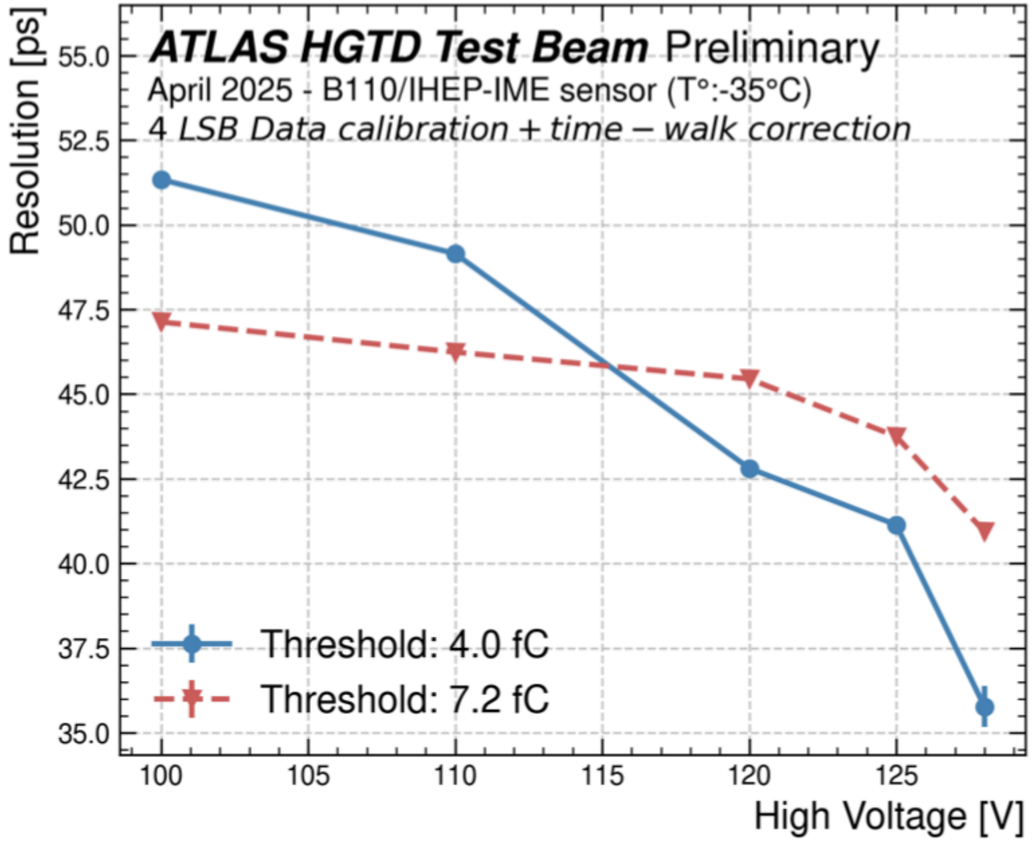

$\Delta t = TOAxLSB - (t_{Clock} - t_{MCP})$

Timing resolution reaches 36 ps

Peripheral Electronics Board (PEB)

- Handles data transmission, LV & HV, monitoring and control
- Main components: lpGBT (data aggregation), VTRx+ (optical), bPOL12V (LV converters), MUX64
- Dedicated data paths for timing and luminosity

- The PEB1F case: 55 FPC, 52 bPol12V, 12 lpGBT, 9 VTRx+, 9 MUX64 within 9.7 mm thickness
- 22 layer PCB, with HDI micro via and VIPPO techniques, High speed, low loss multi-layer material for impedance control

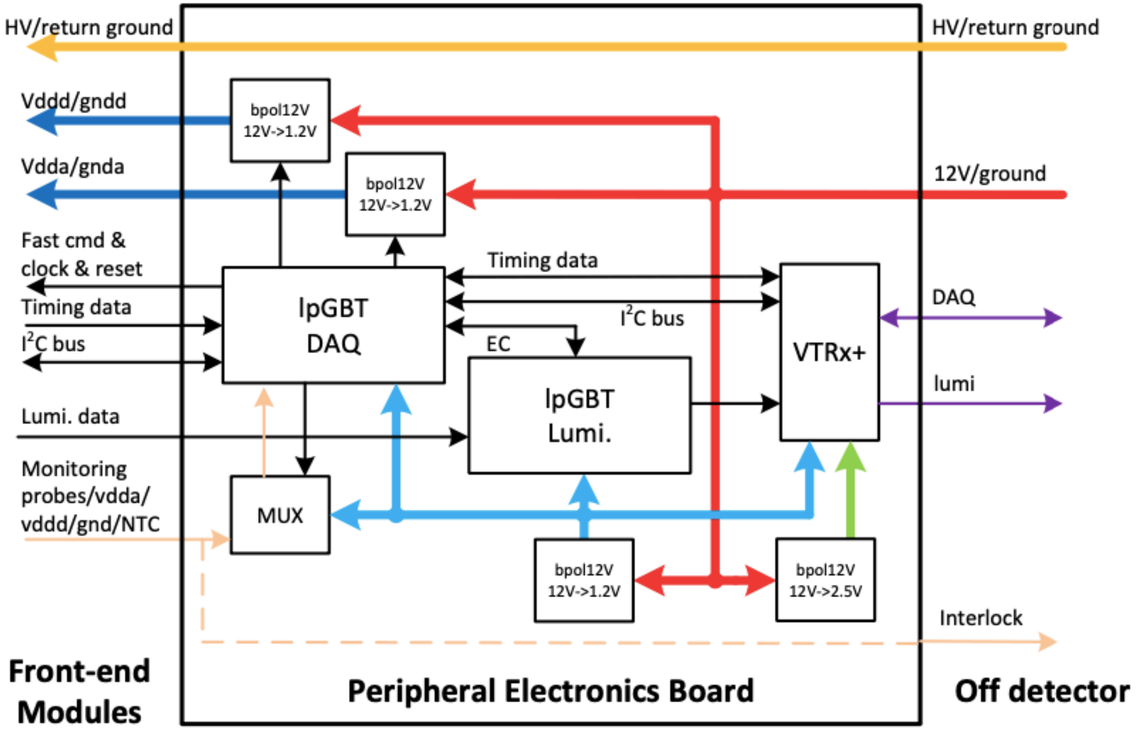

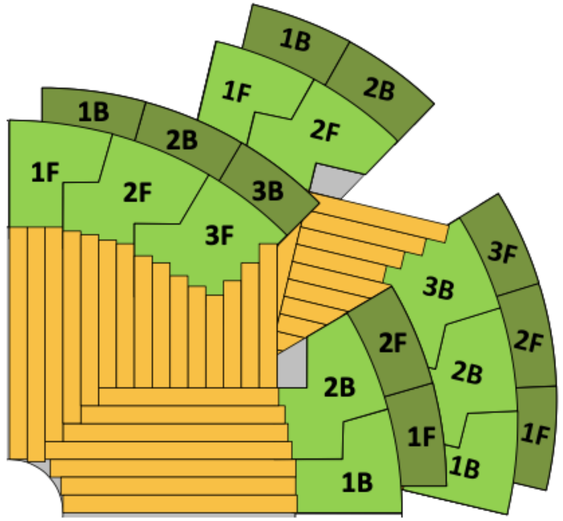

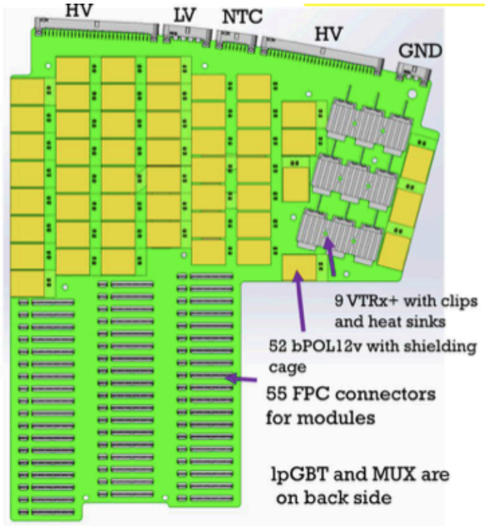

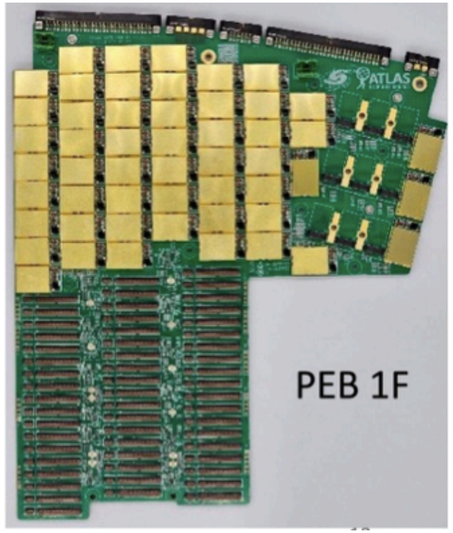

... the most difficult boards manufactured in HEP projects...,

ATLAS P2UG Review committee

The Demonstrator

HGTD Public Results

- Full chain and detector level test with all components.
- One PEB (1F) connecting 54 modules loaded on 4 support units
- LV + HV + PEB + ALTIROC DUs + cooling + DCS&Interlock in a cold box (= -30 °C)
- Allows system-level testing of all components

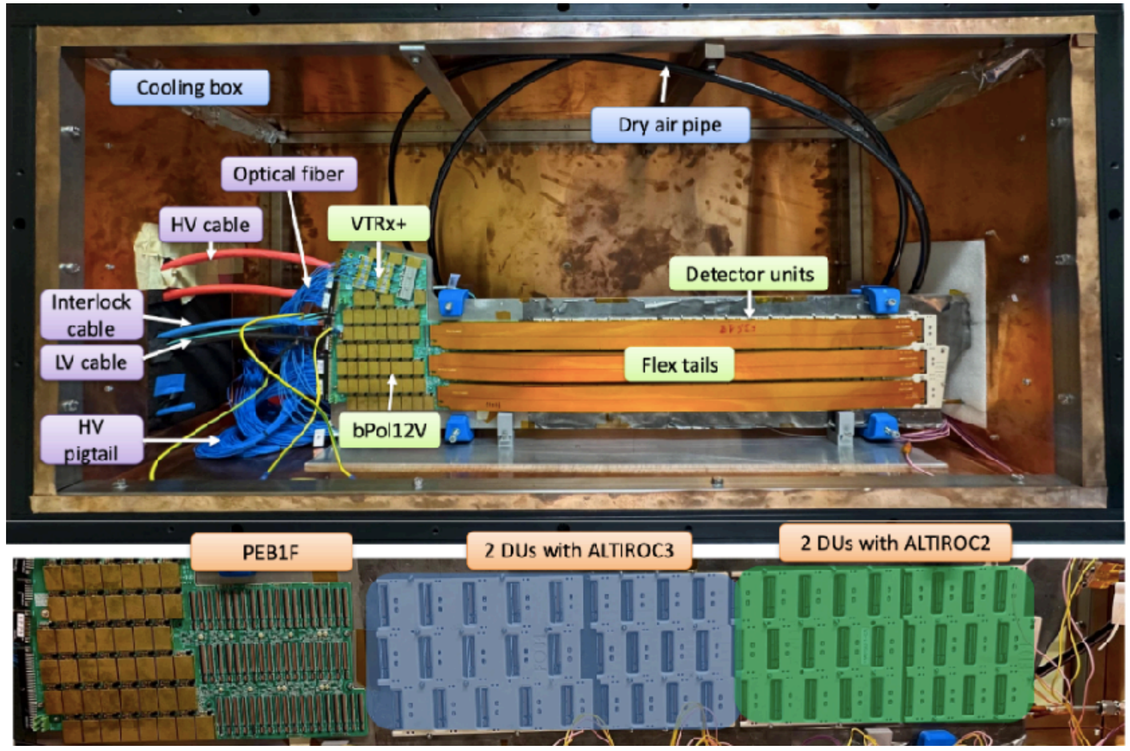

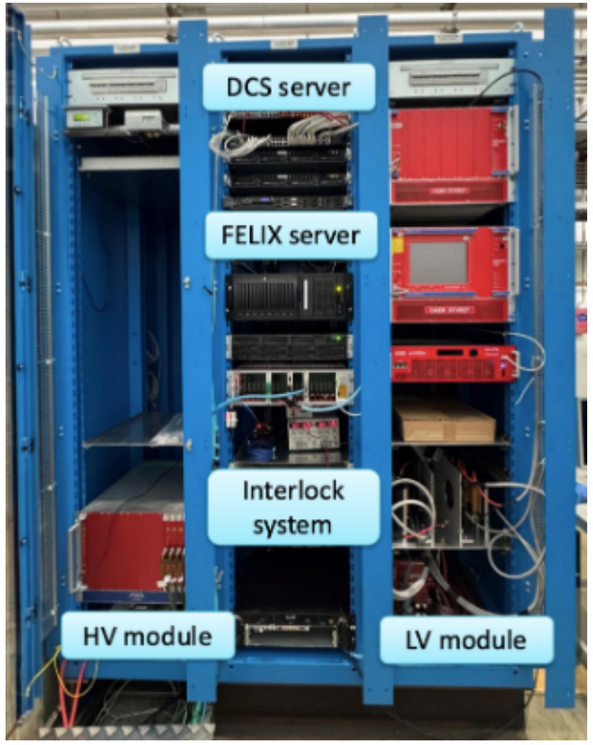

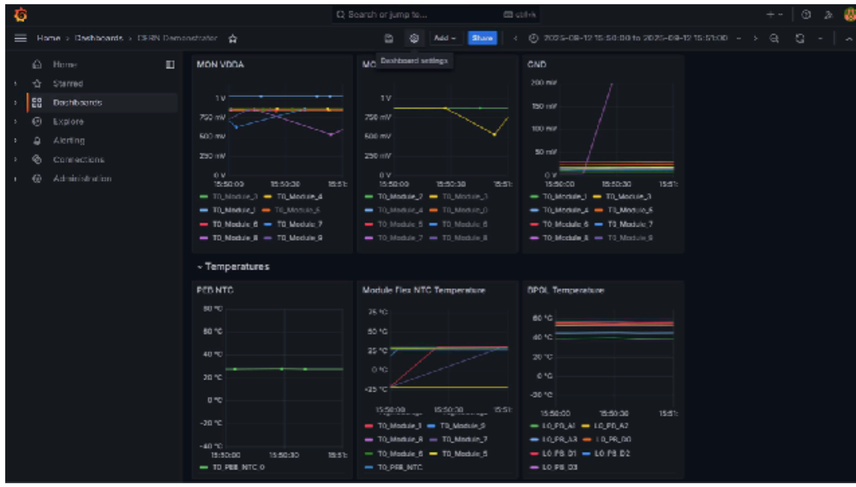

Noise comparison demonstrator/test bench

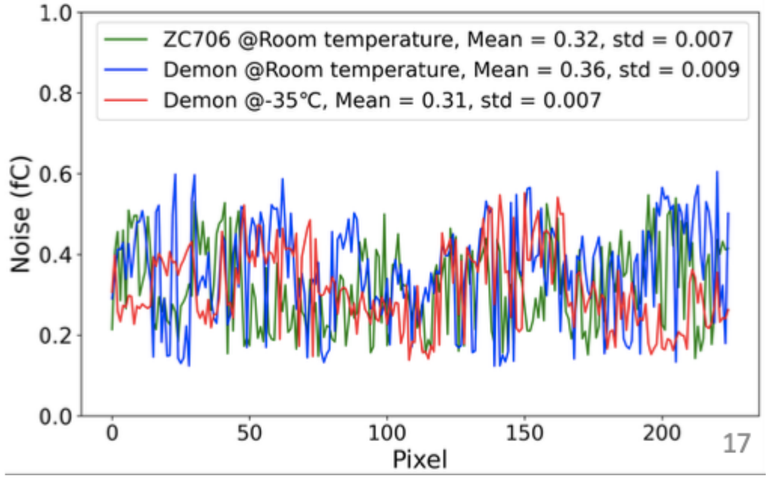

A Module-0 construction (fully integrated prototype consisting in 1/4 disk) will follow in 2026

Luminosity measurement

HGTD Public Results

The high granularity of the ATLAS timing detector ensures an occupancy less than 10%
→ excellent linearity between the average number of hits and ⟨μ⟩ over the full range of luminosity expected at the HL-LHC

The ALTIROC

- Provides per-sensor occupancy per bunch-crossing with 1% accuracy
- Counts hits in every bunch-crossing (40 MHz)
- Has a dedicated readout chain, independent of the trigger and timing data

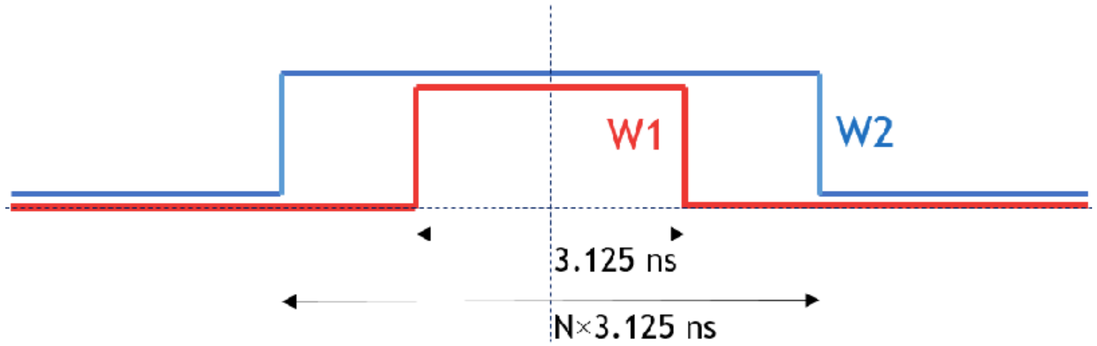

Windows of counting hits centred at the bunch-crossing time
W2 for background correction

Linearity of $\langle n_{hits} \rangle$ as a function of ⟨μ⟩

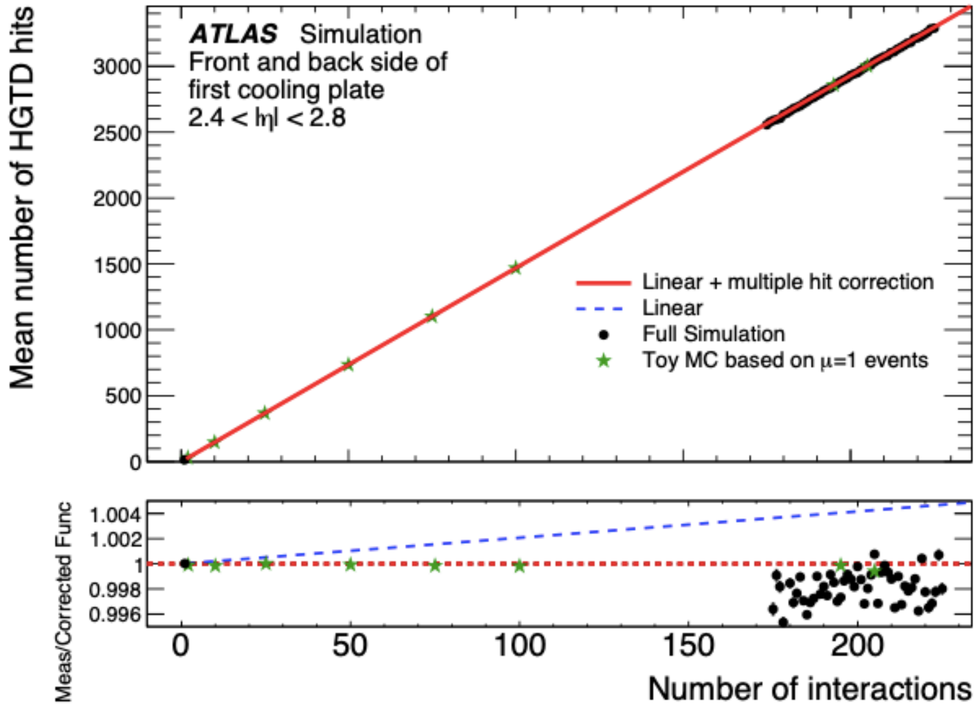

LIP responsibilities

P. Assis, J. Augusto, C. Brito, R. Fernandez, M. Ferreira, R. Gonçalo, L. Lopes, F. Martins, A. Parreira, H. Santos, L. Seabra, R. Vieira

Data Acquisition (DAQ) and Control

- ALTIROC total integrated dose (TID) measurements and functional testing
- Development of Embedded Local Monitor Board (ELMB) carrier boards for CO_2 cooling monitoring

Interlock System

- Responsibility for the complete interlock system

Detector Control System (DCS)

- Control of High Voltage (HV) and Low Voltage (LV) power supplies

High Voltage System

- Patch panel filters
- HV, LV and sensor cables

and in-detector pigtails

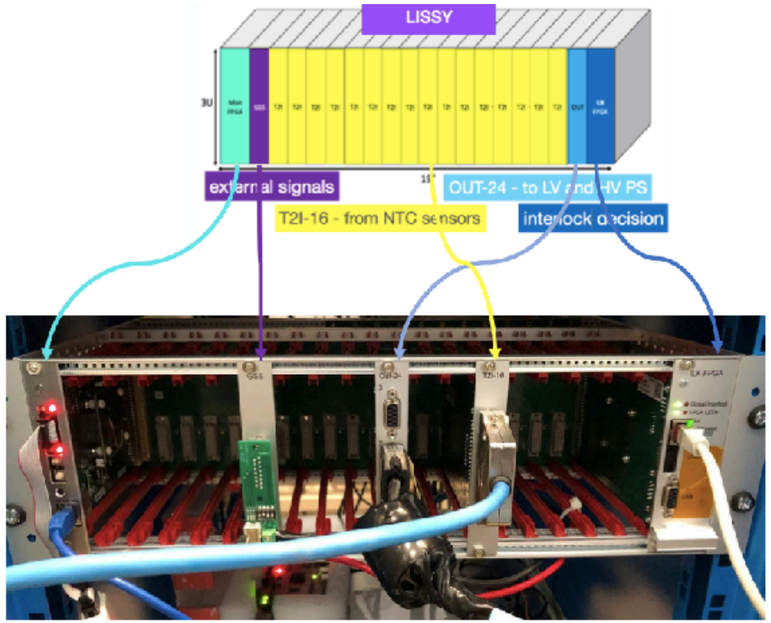

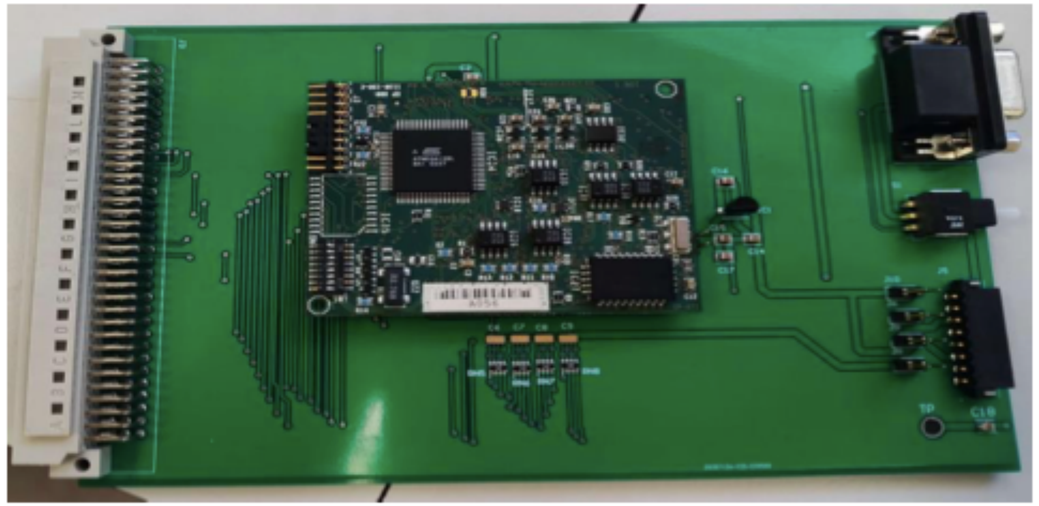

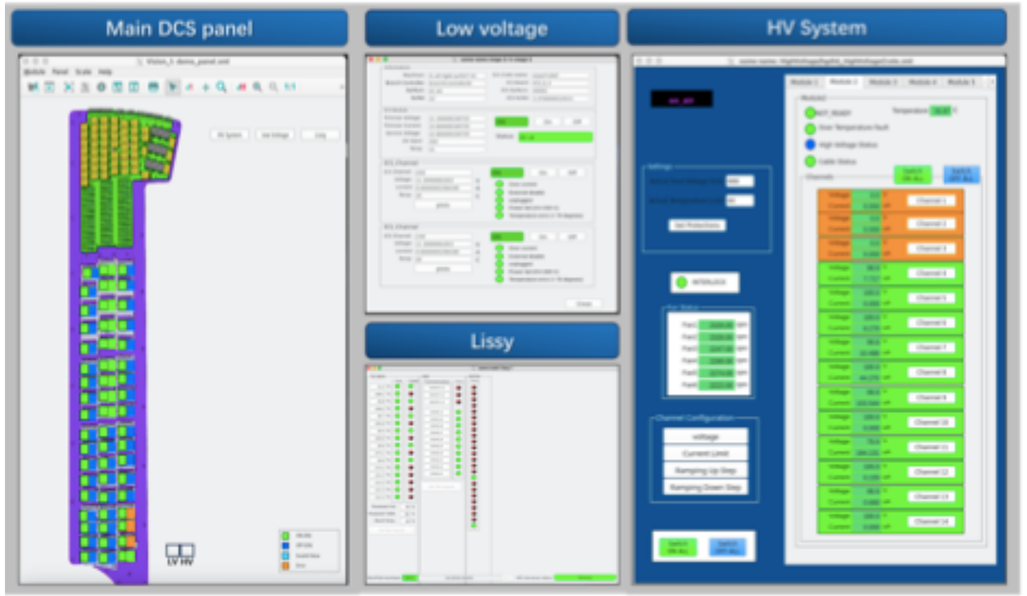

Summary - HGTD performance and status

Per-track timing resolution: 30–50 ps in the forward region, meeting HGTD design targets for precise time tagging of tracks.

It will allow:

- strong suppression of pileup tracks and jets, improving event reconstruction in high-luminosity conditions.
- independent bunch-by-bunch luminosity measurement within 1% precision.

Project status:

- The HGTD is transitioning from R&D to production, with several critical components already under QA/QC.
- A busy construction and integration is ongoing, as we move toward Module0 and full detector assembly and installation.

……Exciting times ahead!

Backup

LHC / HL-LHC Plan

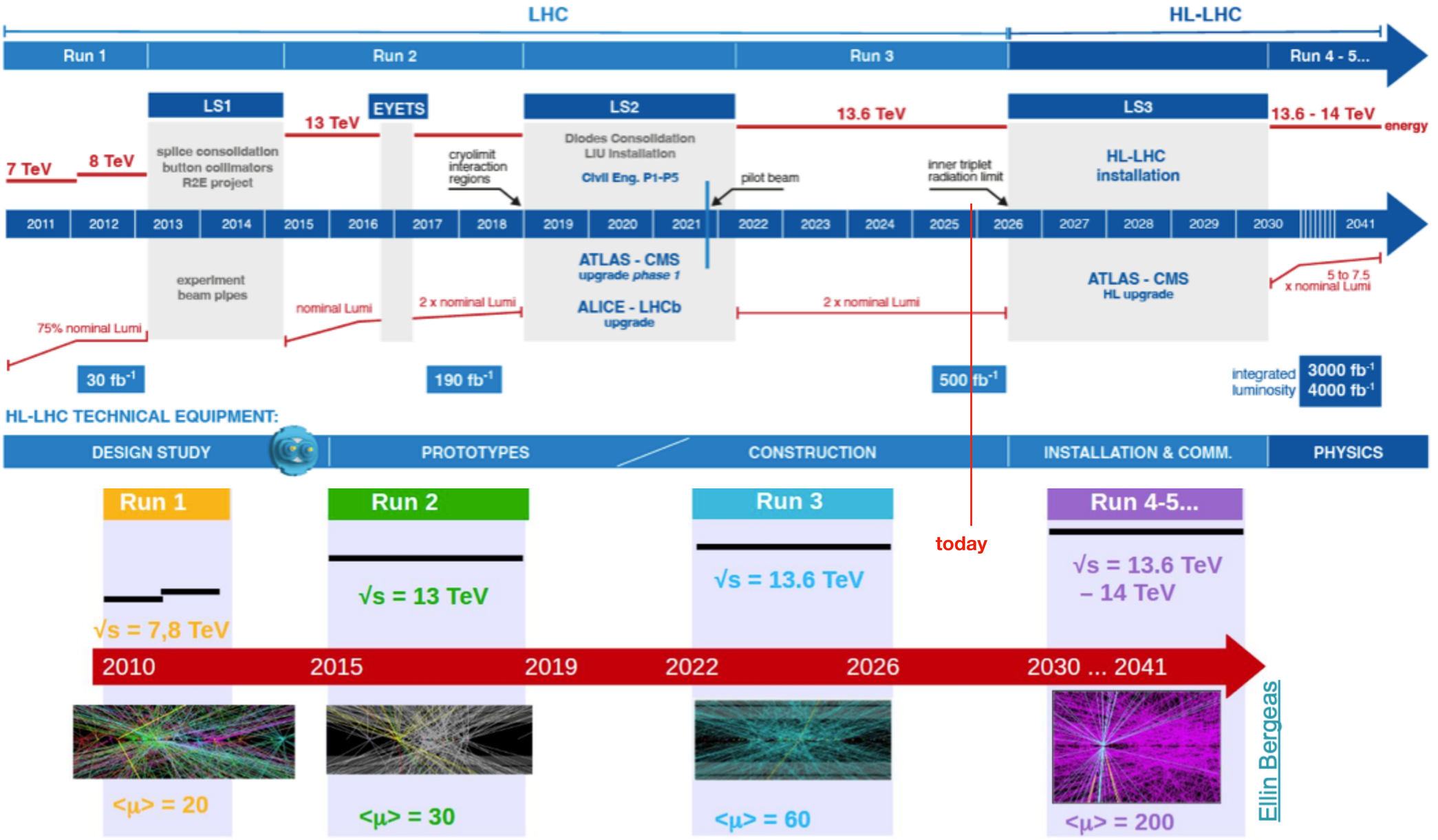

Physics performance with HGTD

HGTD Public Results

Measurement of the weak mixing angle

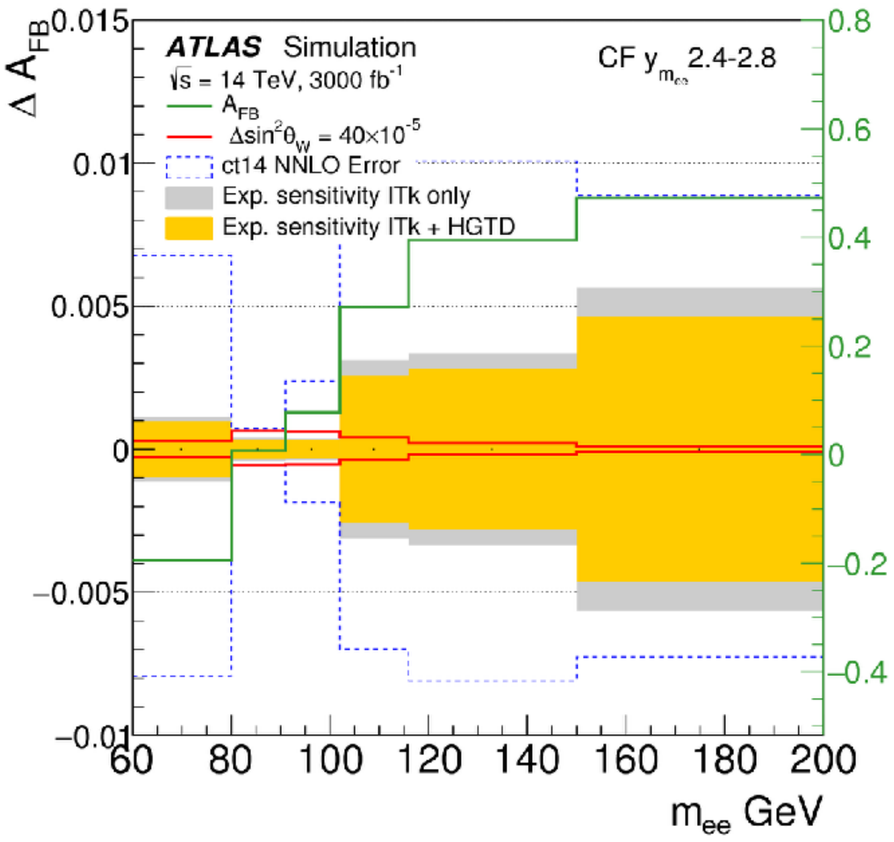

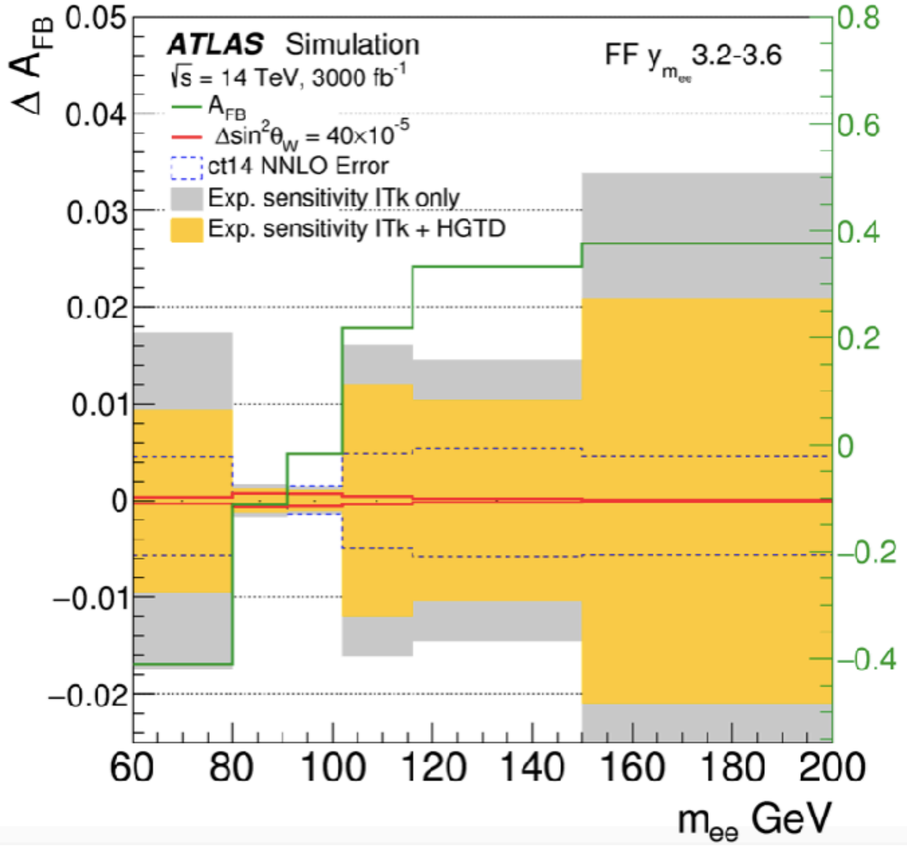

- HGTD enhances the electron–vertex association in the forward region, reducing the uncertainty in the kinematic regions that dominate the A_{FB} measurement
- 13% improvement in the $\sin^2\theta_{eff}$ sensitivity in the Central-Forward channel
- Combining CC, CF and FF, $\Delta\sin^2\theta eff = 18 \times 10^{-5}$ (PDF: $\pm 16 \times 10^{-5}$ | Exp: $\pm 9 \times 10^{-5}$)
  Among the most precise single-experiment measurements.

Intermezzo

Forward physics detectors pioneered R&D in timing detectors - ATLAS Forward Protons and CMS TOTEM Precision Proton Spectrometer

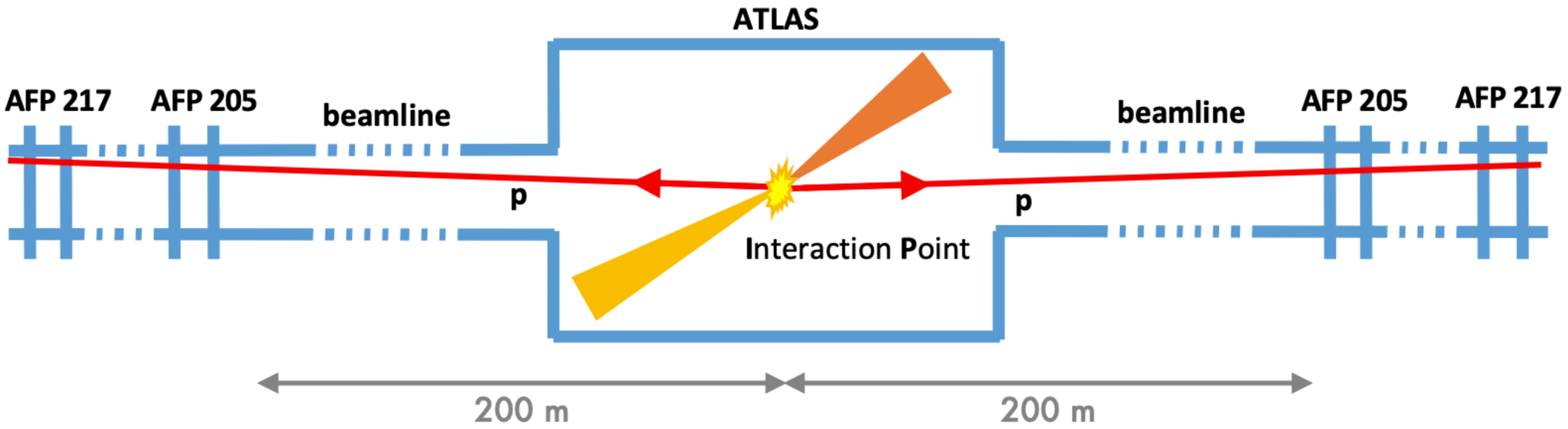

The proton time-of-flight measured in the AFP is used to reconstruct the longitudinal position of the interaction point.

A timing resolution of O(10 ps) translates into a vertex position resolution at the millimetre scale, allowing a direct comparison with the vertex reconstructed in the central detector.

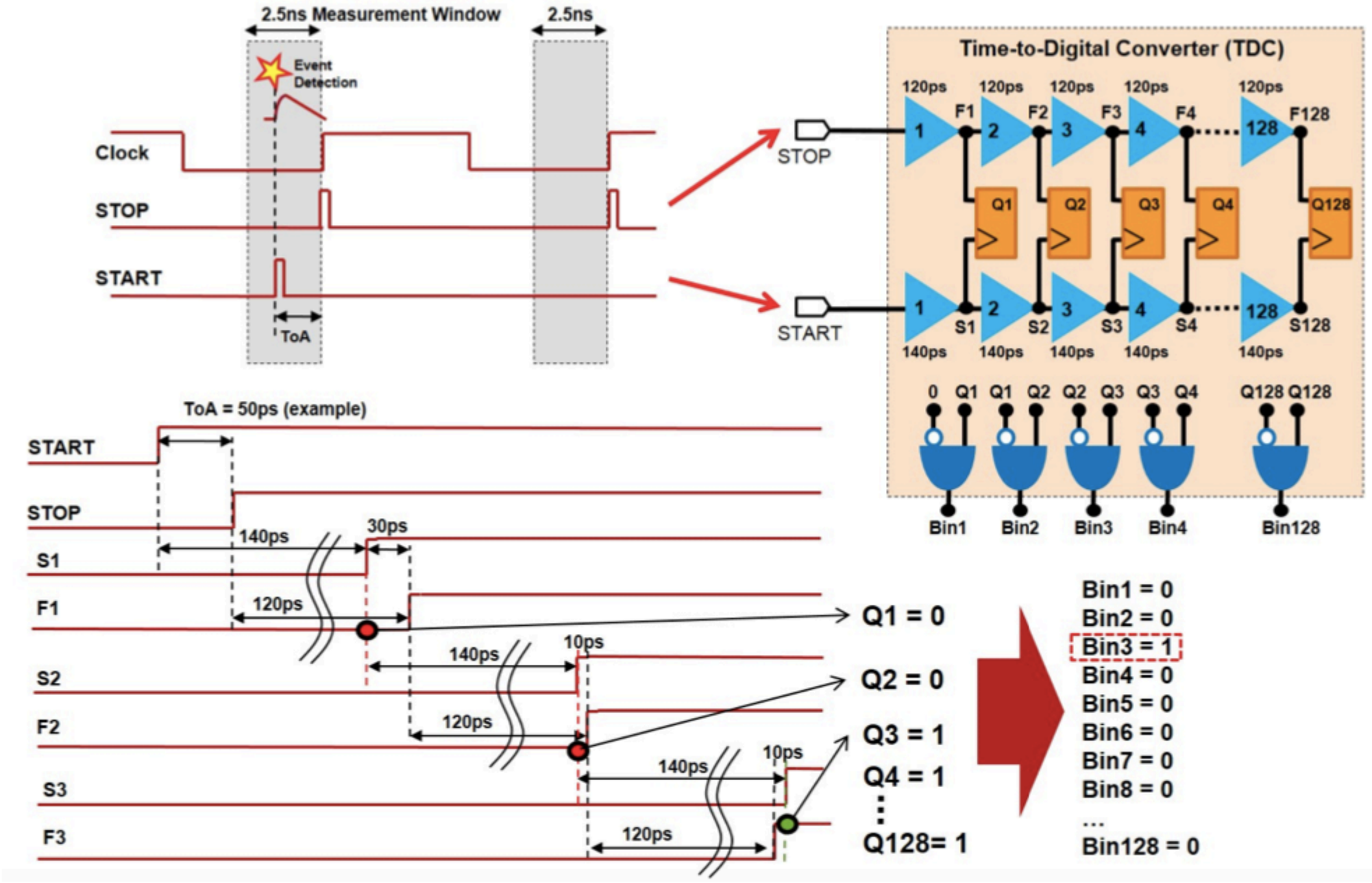
2.5ns Measurement Window
2.5ns
Event Detection
Clock
STOP
START
ToA
Time-to-Digital Converter (TDC)
120ps
F1
F2
F3
F4
F128
1
2
3
4
128
Q1
Q2
Q3
Q4
Q128
STOP
START
S1
S2
S3
S4
S128
140ps
0
Q1
Q1
Q2
Q2
Q3
Q3
Q4
Q128
Q128
Bin1
Bin2
Bin3
Bin4
Bin128
ToA = 50ps (example)
START
STOP
S1
F1
S2
F2
S3
F3
140ps
30ps
120ps
10ps
Q1 = 0
Q2 = 0
Q3 = 1
Q4 = 1
Q128= 1
Bin1 = 0
Bin2 = 0
Bin3 = 1
Bin4 = 0
Bin5 = 0
Bin6 = 0
Bin7 = 0
Bin8 = 0
Bin128 = 0

Irradiation tests - wafer acceptance

NIMA 1084 (2026) 171195

Correlation between most probable collected charge from ^{90}Sr MIP and p-gain layer depletion voltage, V_{gl}, for two sensor designs: IHEP and USTC, both from IME

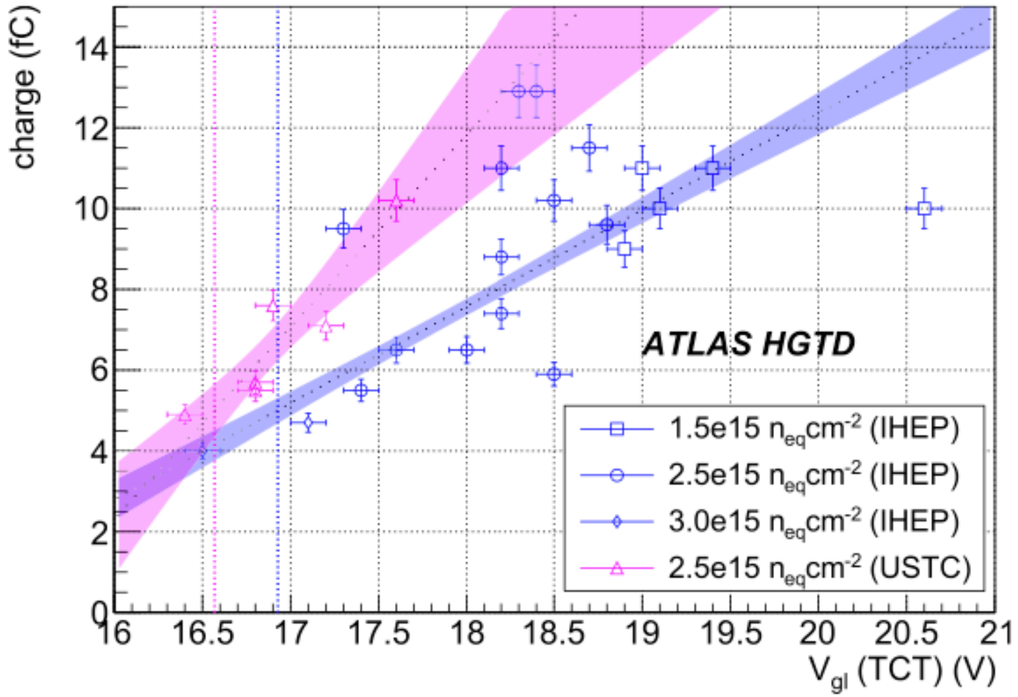

- Several fluences studied: 1.5×10^{15} $n_{eq}cm^{-2}$ and above are shown for the operating voltage at the SEB limit of 550 V
- Data for each design is fitted with a linear fit and uncertainty band represents 1σ fit parameter variation
- The wafer acceptance threshold is defined by the point where the fit intersects a charge of 5 fC (minimum usable signal amplitude)

QC-TS pre-production results

X. Yang

Measurements on ~10 QC-TS per wafer for IHEP-IME and USTC-IME

Gain layer properties

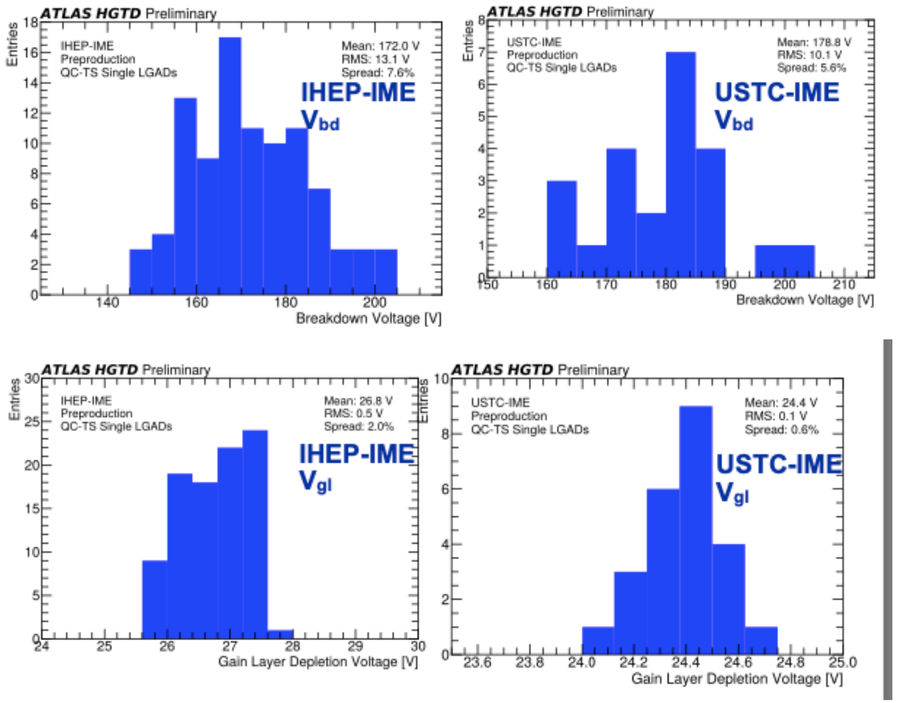

Substrate properties

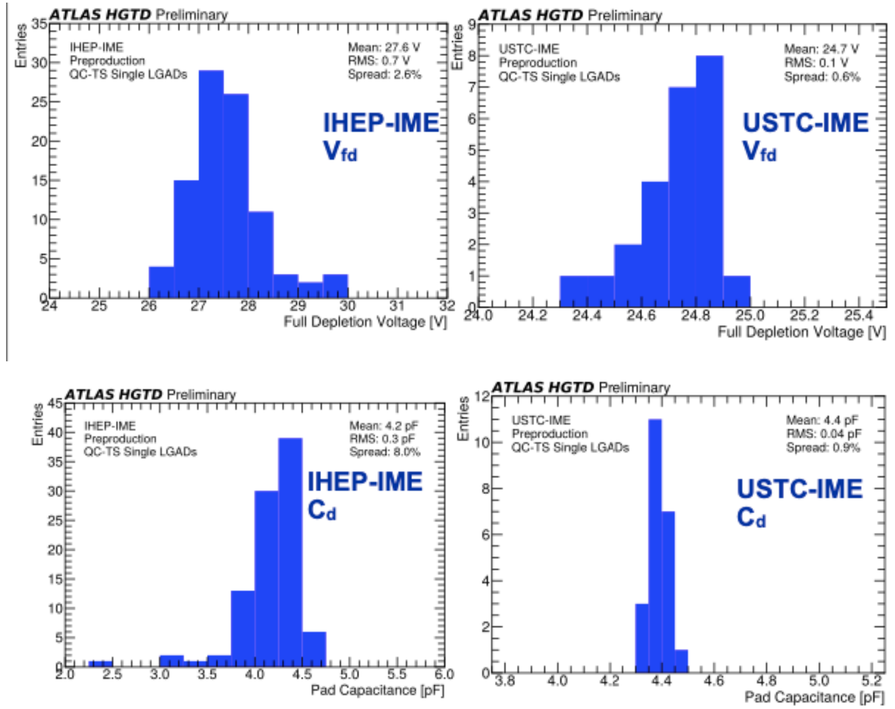

Breakdown of single-pad sensor defined as: V @ 500 nA

- V_{bd} spread:
  7.59% for IHEP-IME and 5.64% for USTC-IME → within specs (8%)

Gain layer depletion voltage:

- Specification: 24V<Vgl<55V with spread 2.02% for IHEP-IME and 0.57% for USTC-IME
  All wafers met the criteria

Full-depletion voltage [V_{fd}]:

- Specification < 70 V —> Spread inside specs (<10%) for both designs
- Resistivity of the substrate is larger than 1kΩ*cm

Detector Capacitance [C_d]:

- Specs: < 4.5 pF —> met

Results consistent within the specifications / expectations

Cooling

HGTD TDR Public Plots